Experimental and Modelling Studies of Gas Solid Vortex Reactor Hydrodynamics

Inês Isabel Antunes Paiva

Thesis to obtain the Master of Science Degree in

Chemical Engineering

Supervisors: Prof. Dr. Ir. Kevin Van Geem

Prof. Dr. Vítor Geraldes

Examination Committee

Chairperson: Prof. Dr. Francisco Lemos

Supervisor: Prof. Dr. Vítor Geraldes

Members of the Committee: Prof. Dr. Filipe Gama Freire

October 2019

Acknowledgements

A cycle has come to an end. I can definitely say these past years were an amazing time for myself, mostly in terms of personal growth. This thesis is the conclusion of that cycle, which could have not ended in a better way.

For that, I must thank to Prof. Dr. Ir. Kevin Van Geem and Prof. Ir. Dr. Geraldine Heynderickx, which allowed this project to become a reality for me. My time in LCT was for sure enriching and pleasant due to my coach, Shekhar Kulkarni, and my almost-coach Manuel Nunez Manzano. Together, they formed the best team I could have asked for my orientation. Beyond their duties, they always showed kindness and consideration towards me. To my two new friends, a major thank-you. A word of gratitude to Prof. Vítor Geraldes for being always available to answer my questions and clarify my doubts. Although being away, he was always at a distance of an e-mail.

My time in Belgium was shared with three amazing housemates. Without them, boredom would have filled my days. To all the laughs and shared memories, I must thank you. A toast to the four of us, we can finally say ‘We did it!’.

To my boyfriend, I express my gratitude for all the patience required along the years and especially during this past few months. For all the challenges already overcome and ones which are coming, I’m sure that there is no better person to have by my side. Love of my life lol.

Finally, to all my friends and family which I left back in Portugal. They are an important part of my life, which I expect to never lose, even if life keeps me away from my home country. To my family which supported my choices and my friends who welcomed me back with a smile and a hug.

Resumo

Esta dissertação tem por objetivo estudar a hidrodinâmica de um GSVR, através da estimativa da sua carga máxima, do grau de mistura/segregação do leito e da avaliação teórica do potencial do reator. A planta piloto opera em regime turbulento (Reynolds de entrada do gás entre 7083 e 10625). Usaram-se métodos experimentais – processamento de misturas com alumina e alumínio (grupos B e D de Geldart, respetivamente), em percentagens mássicas diversas, com diâmetros nominais de 0.7 a 1 mm e com velocidades de injeção de ar entre 56 e 83 $m.s^{-1}$ – e um teórico – modelo matemático. A carga máxima estimada é de 83 gramas de alumina quando a tubagem de escape está orientada contra a gravidade e 30 gramas de alumina para a configuração inversa. Alimentando uma mistura de 75% (m/m) de alumina ao reator, obtém-se 94.4% (m/m) de alumina no leito. A partir do modelo desenvolvido, estima-se, para um reator vazio e para uma velocidade de injeção de 24 $m.s^{-1}$ de ar, que partículas de alumínio com no mínimo 70 μm possam ser fluidizadas, enquanto partículas de alumina devem ter pelo menos 160 μm. A capacidade máxima da unidade é 3 vezes superior quando a tubagem está orientada contra a gravidade, aumentando o caudal de sólidos processado; a segregação de partículas é observada em diferentes graus ao operar o GSVR, reduzindo a necessidade de separação a jusante do reator; e teoricamente a unidade demonstrou potencial em fluidizar materiais dos grupos B e D de Geldart, partículas usadas em diversos processos industriais.

Palavras-chave: GSVR, fluidização centrífuga, segregação de partículas, diâmetro crítico de partícula.

Abstract

The target of the present dissertation is to study the hydrodynamics of a Gas Solid Vortex Reactor, through an estimation of its maximum loading, the degree of mixing/segregation of the solid phase in the bed and a theoretical evaluation of its potential. This setup was built at pilot scale and it's operated in turbulent regime (gas Reynolds between 7083 e 10625). Experimental methods – fluidization of various mixtures with several mass fractions of alumina and aluminium (groups B and D, according to the Geldart classification), with nominal diameters between 0.7 and 1 mm and air injection velocities between 56 and 83 $m.s^{-1}$ – and a theoretical one – a mathematical method – were used. The maximum loading estimated is 83 grams of alumina when the exhaust is orientated against the gravity and 30 grams of alumina for the inverse configuration. Feeding a mixture with 75% (w/w) of alumina results in a bed formed by 94.4% (w/w) of alumina. Using the developed mathematical model, for an empty reactor and an air injection velocity of 24 $m.s^{-1}$, 70 μm aluminium particles and 160 μm alumina particles are the minimum diameter required to achieve successful fluidization. Operating the setup placed in the inverse configuration increases its maximum loading in 3 times, increasing the solids' flow processed; particle segregation is observed while operating the GSVR to several extends, diminishing the need for separation devices downstream; and theoretically the unit showed potential in fluidizing Geldart B and D-type particles, which are used in several industrial processes.

Key Words: Gas Solid Vortex Reactor, centrifugal fluidization, particle segregation, critical particle diameter

Nomenclature

Abbreviations

CCD – Charged Coupled Device

CFD – Computational Fluid Dynamics

CLC – Chemical Looping Combustion

CSTR – Continuous Stirred Tank Reactor

D_{cut} – Critical particle diameter

FB – Fluidized Bed

GSVR – Gas Solid Vortex Reactor

GSVU – Gas Solid Vortex Unit

HDPE – High Density Polyethylene

HPC-L – Hydroxypropylcellulose

IR – Infrared (camera)

LCT – Laboratory for Chemical Technology (located in Gent, Belgium)

MIVR – Multi Inlet Vortex Reactor

PI – Process Intensification

PIV – Particle Image Velocimetry

PLIF – Planar Laser Induced Fluorescence

RFB – Rotating Fluidized Bed

SPIV – Stereoscopic Particle Image Velocimetry

SNAP – SO_2 and NO_x Adsorption Process

w.r.t. – with respect to

Symbols

Latin Alphabet

A	Area	m^2
C_D	Drag Coefficient	-
D	Diameter	m
F	Force	N
$F1$	Fraction of larger particles	-
$F2$	Fraction of smaller particles	-
G	Gas flow rate	$m^3\ h^{-1}$
H	Height of a GSVU	m
I_N	Number of slots	-
I_0	Opening of the slot	mm
L	Length	m
m	Mass	g
P	Pressure	mbar
R	Radius of a GSVU	m
Re	Reynolds Number	-
r	Radial position	m
S	Swirl ratio	-
u, v	Velocity	$m\ s^{-1}$
W	Capacity	g

Greek Alphabet

α	Slot angle	-
ε	Void fraction	-
θ	Angular coordinate in a GSVU	-
μ	Dynamic viscosity	Pa s
ρ	Density	kg m^{-3}

Subscripts

C	Centrifugal
cut	critical
D	Drag
f	Fluid
g	Gas phase
max	maximum
p	Particle
r	Radial component
s	Solids, slots
θ	Tangential component

Table of Contents

Index of Figures

Index of Tables

1. Introduction

Gravitational fluidization is a process applied on binary systems, e.g. gas-solid systems. Literature about the subject appears on the late 1940's[1,2]. Studies about mixing of both phases[1] and the hydrodynamics of the process[2] arise as the referred technology becomes known and interesting for the scientific community. This technology showed to be useful for catalyzed reactions, where the catalyst is usually the solid phase and the reactional mixture is the gas phase, and to control the reactor temperature when the reaction is exothermic. As expected, while a bed is fluidized, a large surface area between the solid phase and the gas phase is obtained, increasing the heat transfer coefficients of the system, promoting a higher uniformity of the results and avoiding hotspots.

Although having many advantages and applications, classical fluidization cannot handle particles with extreme small sizes, such as nanoparticles. The characteristics of the particle can also be damaged during the entire process, since collisions with the walls and between particles happen. As a result, the particle can break, if the material is fragile (for example ceramics). The opposite can also happen. Particles can aggregate, modifying the size distribution of the solid phase, decreasing the uniformity of the results. The pressure drop associated with fluidization is an important aspect. At an industrial scale, pressure drop can easily achieve higher values, provoking large fluctuations between inlet and outlet pressure. As a result, this process demands powerful (and therefore costly) compressors[3]. The most important limitation of classical fluidization is the terminal velocity of the solid phase. This variable cannot be changed using gravitational fluidization since gravity has approximately the same value on every position of the setup. This implies that there is a limit to what can be achieved using this technology[4].

Such limitation can be overcome by using centrifugal fluidization. Such technology has been studied since the 1960's[5], but it hasn't reached the industrial world yet. In this case, the fluidization is achieved by transferring the gas phase momentum to the solid phase, causing the latter to rotate inside the chamber, generating a bed close to slot walls. As the transfer happens, the gas loses its momentum to the solid phase, inducing a change in the velocity of both phases. In centrifugal beds, the centrifugal field can assume different values and can easily reach high values, depending on the fed gas flow rate. Therefore, terminal settling velocity does not have a defined upper limit, making the potential of such technology much wider than classical fluidization[4].

There are at least two types of reactors where centrifugal fluidization happens: Rotating Fluidized Bed's (RFB's) and Gas Solid Vortex Reactor (GSVR). They differ in the chamber itself and the technique used for fluidization. For the first case, there is a motor that allows the chamber to rotate on an axis and it is typically operated horizontally (i.e. with vertical axis). In the second one, every part is static, and the solids only have azimuthal motion thanks to the air that is fed to the reactor through several slots[4]. The RFB has become obsolesce, since moving parts mean higher costs, related with electricity, which powers the motor, and maintenance, since such parts get rapidly damaged and need to be replaces often. Hence, GSVR's have been gaining more attention from the industrial world and the scientific community. Regarding operational conditions, a GSVR is easily operated. Experiments

can be done in a short period of time. Cleaning the solid phase is also an easy task. All things considered, this reactor is easily operable.

Centrifugal fluidization has a wide range of applications. Industries like food processing, fuel production, and biomass processing are investing on possible ways to incorporate this type of fluidization on their processes[6-8]. The drying of chilies in a rotating fluidized bed device[6] is reported has a possible application of RFB. Using the rotating fluidized bed technique makes the process easier to be controlled and presents much better results when compared to natural drying, such as less duration time and a lower operational temperature. Feeding natural gas into a vortex flow reactor and exposing it to the sunlight leads to a carbon and hydrogen generation (the ruling reaction is $CH_4 \rightarrow C + 2H_2$)[8]. Since there is no flame or burning of any kind, there are no oxides, namely CO_2, formed. Therefore, the carbon obtained is free of impurities. It also offers the possibility of storing and transporting solar energy[8]. An experimental comparison between the drying of biomass under gravitational and centrifugal forces is also present in the litearture[9]. To compare the performance of both systems, a process intensification factor is established. Using the centrifugal technology and in terms of the specific drying rate, it was possible to intensify the process by one order of magnitude.

Analyzing the reported examples, the concept of Process Intensification (PI) arises. The aim for greener processes and the demanding policies in what concerns industrial processes are aspects which become more and more important every day for any chemical industry in the world. Using the definition proposed by Stankiewicz and Moulijn, PI is '*Any development that leads to a substantially smaller, cleaner, safer, and more energy efficient technology*.'. The level of improvement that is expected when a process is submitted to intensification must be considerably high since the modifications done imply questioning and adapting processes that were used for decades.

The vortex technology is an example of a process intensifying equipment since the heat and mass transfer coefficients are largely improved when this equipment is used. Such variables are related to the driving force of processes like drying, one of the main applications of GSVRs. Those improvements are mainly due to mechanical changes. The reactor geometry (the feeding of the gas phase and the chamber itself) leads to centrifugal fluidization, improving the chemical variables of the process, such as the yield of the process or the drying time. Besides, the size of the unit can be quite small when compared to gravitational technologies, since the residence times of both phases are considerably smaller under centrifugal forces. Particle segregation, a phenomenon reported on the literature[10], can perhaps replace or diminish the need for separation devices downstream. Hence, there are a lot of aspects of a GSVR which can contribute to PI, making this technology worth to study.

After contextualizing the GSVR technology attending today's industrial world, the scope of this dissertation arises. More studies must be made and documented on the subject so that industry comprehends the true potential of this technology. The construction of a mathematical model capable of assessing which particles (using their size and density) can be successfully fluidized in a certain GSVR is the first objective to be discussed. A force balance to a single particle will be performed and iterative method will be used for solving the resulting equation. Evaluation of the possible configurations on how the setup can work, establishing the most efficient in terms of maximum loading is one priority.

For that, alumina particles will be fluidized with air (injection velocities between 56 and 83 $m.s^{-1}$) when the setup is placed against gravity. The results of the same experiment but with the inverse configuration have already been reported by another student[11]. The results from both students will be graphically presented. Estimation of the extent of the particle segregation and how it can be used to enhance a process is the last goal to be discussed. To achieve that, particles from several materials and sizes will be mixed and fluidized using several air injection velocities. The outcoming bed will be analyzed, using size as a separation factor and measuring the amount of each material present in it. That ratio between the two different groups of particles will tell the extent of segregation/mixing in the bed, for a specific mixture. Accomplishing all these objectives means that a significant quantity of information will be collected, helping researchers to apply centrifugal fluidization on their works.

2. Literature Review

This chapter will include a complete description of a Gas-Solid Vortex Unit, its fundamentals, advantages and disadvantages of such technology, industrial applications and some promising processes that were only developed up to a pilot scale. Some characteristics of this unit which are recently investigated, such as segregation of particles with different sizes or densities will be explained and its subsequent value to the industry and feasibility discussed. The fluidization of Geldart A- and C-type particles, which are used as catalysts and for coating, in centrifugal reactors and some techniques to deal with such challenging particles when it comes to fluidization will also be explained and enumerated. The fluidization behavior under gravitational and centrifugal forces of such particles will be compared under the scope of what forces are responsible for the flowing pattern often presented by such particles once they are fluidized and how one can improve the fluidization quality of these materials. Examples of re-interpretations of the Geldart chart presented in the literature will also be provided, with the intention to guide a researcher on how to plan the construction of a new classification for gas fluidization of solids under a centrifugal field. Within this review, the topic of process intensification will also be explained, since this concept is strongly associated with centrifugal fluidized beds.

2.1. Gas-Solid Vortex Chamber – a unique technology

2.1.1. Fundamentals

A Gas-Solid Vortex Reactor is a relatively new technology that allows the gas fluidization of solid particles in the form of a rotating fluidized bed in a static unit. Although it's worth has been proven in literature, its industrial use is still narrow, mainly because there is still a lack of knowledge on how to do the scale-up of this type of units. The lack of correlations to describe accurately the main aspects of such units, related to heat and mass transfer, also contributes to its limited use[12].

These units fall under the group of centrifugal fluidized beds. These beds are not only under the influence of a gravitational field but also under a centrifugal field, which changes the way particles with a certain diameter and density behave when they are fluidized. Subcategories of centrifugally fluidized beds contain the rotating fluidized beds (RFB's) and vortex fluidized beds. They differ in the chamber itself and the technique used for fluidization. For the first case, there is a motor that allows the chamber to rotate on an axis and it is typically operated horizontally (i.e. with vertical axis). In the second one, every part is static, and the solids only have azimuthal motion thanks to the air that is fed to the reactor through several slots.[4] The number of slots of the reactor influences the inlet velocity of the gas phase, for a given flow rate, and consequently the stability of the bed, since the distribution of the gas phase will be more uniform among the bed. The dissertation will be focused on the static chamber design.

The rotating bed is obtained only because of the momentum transfer from the gas to the solids since all parts are static. Due to the momentum transfer from the tangential velocity component of the gas, the solids inside of the chamber rotate. The radial component of the gas will attempt to drag the particles towards the exhaust which is located at the central axis of the reactor. The tangential component of the gas will force the solids into a circular motion which causes a centrifugal force to

counteract the radial drag force thus creating a rotating fluidized bed[13]. Using this technology and until now, it's only possible to change the inlet velocity of the gas phase. Inside the reactor, one does not have control over each velocity component (both tangential, $u_{\theta,g}$, and radial, $u_{r,g}$) and therefore the swirl ratio, S, is constant for a given unit configuration, e.g. for a certain arrangement of the slots[14],

$$S = \frac{u_{\theta,g}}{u_{r,g}} = \frac{2\pi R cos(\alpha)}{I_N I_0} \quad (1)$$

Where R is the chamber radius, α is the slot angle, I_N is the number of slots and I_0 is the opening of the slot.

In this type of units, the fluidization is achieved by transferring the gas phase momentum to the solid phase, causing the latter to rotate inside the chamber, generating a bed close to slot walls. As the transfer happens, the gas loses its momentum to the solid phase, inducing a change in the velocity of both phases. Hence, as the gas flows along the reactor until the exhaust, its velocity diminishes, and the solids gain velocity as they travel radially inwards inside of the chamber.

The fluidization inside such units is believed to happen layer by layer, which is significantly different from the mechanism that rules the fluidization under gravitational fields. Under these circumstances, the particles located nearest the slot wall of the unit are the first to be fluidized, since they are the first to contact with the gas phase coming from the slots. Increasing the gas flow rate, the consecutive layer will also be fluidized, since the momentum of the gas phase increases. The gas flow rate should be increased until all the solids are rotating. The gas flow rate which allows the fluidization of the entire solid phase is called critical fluidizing velocity[15]. However, despite the changes in fluidization, the pressure drop behavior with respect to the gas velocity for a centrifugal system is the same as the one for gravitational ones.

Partial fluidization is a phenomenon connected with vortex units, being one of the necessary steps to achieve fluidization of the entire bed[16]. Such effect is linked with expanded bed heights and a larger radius of the chamber. Partial fluidization involves the presence of two layers in the solid phase. The layer close to the walls is in the packed-bed region and the consecutive layer is in the fluidized-bed region since the fluidization commences in lower radial positions[17].

Such process happens when the gas velocity increases up until a certain value and the centrifugal force decreases due to a smaller radial position. At this stage, particles with the smaller radial positions, where the centrifugal force is smaller, start to fluidize. Once the gas has enough momentum e. g. reaches a certain velocity, it overcomes the centrifugal forces acting on the particles near the slots and therefore the whole bed becomes fluidized. This step is part of the set of crucial stages to achieve fluidization in a rotating bed. They are, by chronological order, fixed bed, partial fluidization, partial bubbling, uniform bubbling and, finally, turbulent fluidization[17].

Layers of different particles which lay inside of the vortex unit will be mixed at some point. If those particles have the same density, mixing will happen because of bubbling. For particles with different densities, this mechanism suffers some changes. If the denser particles are nearest to the slots, the

mechanism does not change. If that is not the case, mixing will happen before bubbling, just due to the difference of densities. Remark that bubbling still happens but does not imply mixing and both phenomena are not linked.

Operation in such equipment is not limited by the gravitational field as in a classical fluidized bed since the centrifugal force must be considered. Therefore, there are 3 forces acting inside of the reactor: the gravitational, the drag and the centrifugal, represented in Figures 1 and 2. In the gravitational fluidization, the velocity of the solids is limited by their terminal velocity when subjected to a gravitational field, which value is constant. This implies that there is a limit to what can be achieved using this technology. In centrifugal beds, this limitation can be easily overcome because the centrifugal field can assume different values and can easily reach high values. Therefore, terminal settling velocity does not have a defined upper limit. Since the centrifugal field can assume different values for each radius, the concept of minimum fluidization velocity for a certain set of conditions is not totally applicable in centrifugal fluidized beds. A minimum gas flow rate is, however, required to achieve high-G operation [4]. The mentioned forces acting in a centrifugal reactor are depicted in Figure 1 and Figure 2.

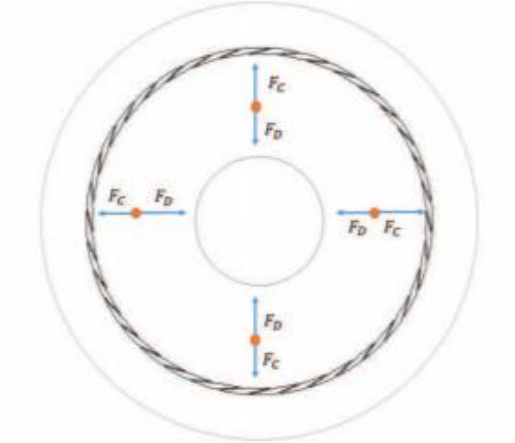

Figure 1. Plant of the forces acting in a centrifugal fluidized bed (reactor orientated vertically).

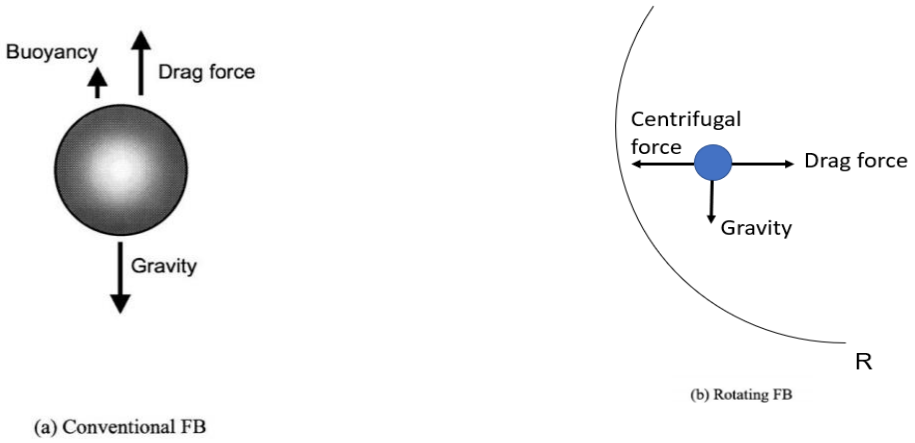

Figure 2. Comparison between fluidization mechanisms [18]

Higher slip velocities between the solid and the gas phase are desirable because it allows achieving higher mass, momentum, and heat transfer coefficients, improving the contact between the two phases. Many studies[7,19] also claim that for denser beds the gas-solid interphase area per unit of volume will be larger, and therefore, the transfer coefficients will also be larger. This is the main reason why centrifugal beds are gaining importance in chemical processes, mainly in process intensification.

Because of the centrifugal force, instigated by the rotating bed, the force field is much stronger than the one acting on classical fluidized beds. Centrifugal forces up until 278 times the gravitational are reported in the literature [20], but for continuous operation, the limit reported in the literature is 40G[4]. Overcoming that limit for continuous processes would lead to higher gas phase consumptions and shear in the particle bed [4].

Although the given information, GSVR's can process higher gas flow rates without influencing the quality of the fluidization. In fact, increasing the gas flow rate fed to a GSVR can even improve the quality of the fluidization. If an excess of gas is fed to a system where classical fluidization is aimed, it is probable that channeling and bubbling will be observed in the bed, because of gas bypassing. As a consequence, the quality of the fluidization will be negatively affected. Under centrifugal fields, an excess of gas will not cause the mentioned phenomena on a significant scale. Actually, the rotating velocity of the bed will increase and the contact between the present two phases will be enhanced. Therefore, the quality of the centrifugal fluidization will also be improved[15]. Other studies[17] support this theory but claim that the influence of the bed height is not clear, and more studies should be done on the topic.

2.1.2. Advantages and Disadvantages

Using any type of fluidization as a technique to handle multiphase systems has its advantages and disadvantages[3,4,9,21].

As expected, a large surface area between the solid phase and the gas phase is achieved using this technology. The high thermal inertia of the solids is another characteristic of this regime, which is important because it measures the tendency of a material to hold heat. Therefore, solids with higher thermal inertia will keep the same temperature for a longer time. This is an important feature because it reduces the amount of heat to provide to those particles for them to keep a certain temperature. An improvement of the solid phase mixing degree leads to more uniform results and helps to avoid hotspots. With fluidization, the transfer rate of water and heat becomes faster, decreasing the drying time without subjecting the solids to high temperatures, which can cause permanent damages. Transporting the solids in and out of the dryer by pneumatic transport (a further stage of fluidization) means less mechanical and energetic costs.

There are also some undesirable consequences related to fluidization. If the solids used are fragile, the attrition and the friction can lead to the breakage of the solid phase, to the point of pulverization. Those fine particles will most likely be lost in the exiting gas stream. Another scenario is the aggregation of the fines, leading to a serious change in the size distribution present in the unit. Consequently, the drying rate will diminish, and the results will be less uniform and possibly worse than expected. The residence time distribution is affected when fluidization is used. Because of the higher mixing degree, the residence time distribution will increase. Regarding the lifetime of the device where the operations take place, these are more exposed to erosion, leading to the wear of the facilities, that should be replaced often. Pressure drop is often associated with fluidization systems since, for gas-solid systems, the gas phase loses its velocity when going through the solid phase. That pressure drop increases with the increase of the gas velocity, until a certain limit. Most of the times, that limit is high enough to cause serious differences in the inlet and outlet pressure. Hence, fluidization is a demanding process when it comes to compressor costs. The higher the pressure drop of a system, the powerful the compressor associated needs to be[3]. For larger bed diameters, the distribution of the gas phase over the bed is delicate. If the distribution system is not built in a proper way, phenomena as channeling and slugging can happen. Both are related with an unstable bed behavior. Channeling is the formation of preferential paths for the gas phase, which leads to poor fluidization. Slugging is the aggregation on solids in several parts of the bed, making the bed surface non-uniform.

For classical fluidization, fluidizing sub-micron particles is difficult and sometimes impossible, since the Van der Waals forces for such small particles are extremely strong and overcome the interfacial momentum of those particles. On the other hand, in an ideal fluidized bed without cohesive forces, a stable bed is not achievable[20]. This technique is not flexible. In order to obtain a stable bed, the system must be designed specifically for that material and the operating conditions cannot differ much from the minimum fluidization ones. To avoid channeling and slugging, the ratio between the bed width and height cannot be changed from a calculated value[4]. Another concern is the wall effects that often influence the quality of the fluidization. In RFB's, those effects are negligible[17].

Some of these limitations can be overcome when operating under centrifugal forces. A rotating fluidized bed allows having a more efficient control on the residence time of the solids[9]. Besides, a wider range of residence times is allowed in such units. Regarding slugging and channeling, these phenomena

can still occur but since the width-height ratio of the device is usually smaller, they are less likely to happen[4]. The flexibility of operating conditions with respect to the gas flow rate is increased when centrifugal fluidization is used, but the unit needs to be wisely designed to achieve the balance between the centrifugal and drag forces. This balance is mandatory to avoid the entrainment of particles into the exhaust at the same time to achieve a denser and stable bed. Another advantage is the possibility of controlling independently the gas and solid flows over a relatively wider range.

Although there seem to be many disadvantages related to fluidization, these aspects are related to very specific operating conditions. There is still a very wide range of conditions which can be explored. The disadvantages that are common to most systems can be minimized using a centrifugal fluidization unit, as the case of channeling and slugging, which can be more accurately controlled using this technology. The worse aspect is perhaps the damaged inflicted in the dryer and the vessels connected to that, but the results achieved largely compensate for those costs. The need for larger gas volumes, and therefore, larger chamber volumes is also a disadvantage. Higher capital costs are associated with this characteristic. However, such condition can be overcome by choosing reactive systems, especially where the gas phase is consumed during the reaction.

2.1.3. Measurement Techniques

In a GSVR several properties must be measured to ensure a good set of operating conditions. In a non-reactive and in a hydrodynamics prospect, the solids velocity, gas and solid temperature pressure are some of the most important variables. Along with these variables, heat transfer characteristics of the reactor/unit need to be established by using above mentioned variables. This section is therefore dedicated to summarizing some measurement techniques that can be applied in a GSVR. A comment is also added regarding heat transfer in vortex devices.

Solids Velocity and Flow Pattern

When dealing with fluids, liquid or gas, traveling inside a reactor or a chamber, its flow pattern and flow dynamics should be analyzed. Therefore, quantitative measurements of its properties, namely the position of each particle along time, velocities of particles as a function of radial positions, etc. are required. For that purpose, many researchers use Particle Image Velocimetry (PIV) techniques.

PIV is a 2-dimensional optical technique that allows to characterize the azimuthal velocity field of the fluid or the solid phase in a certain region of the chamber. A typical PIV setup consists of a Charged Coupled Device (CCD) camera, high power laser, an optical arrangement to convert the laser output light to a light sheet, tracer particles and the synchronizer. The laser and the optical arrangement that follows illuminate the area which will be examined. The laser has therefore two purposes – illuminate the examined area and avoid the blurred images, since they freeze the solids' motion[22]. With the CCD camera, a pair of images is taken, which have apart only a few moments. As a good practice, the gap between two pictures should be enough to let the particle move a quarter of the final interrogation area[23], which is a portion of each image taken by the camera[24] . On the other hand, that gap should be short enough so that the particles with an out-of-plane velocity component leave the light sheet[22]. After both

shots are taken, the displacement of the particles and the time in between those pictures are used to calculate the particle velocity and therefore, to build a 2D particle velocity vector field[23]. The information contained in the images can be converted in a text file, which contains the spatial coordinates and information regarding the components of solids velocity. That information can afterwards be processed using a programming software. Finally, the synchronizer is used to coordinate the laser with the CCD camera[25]. All the procedures involved during PIV are summed in Figure 3.

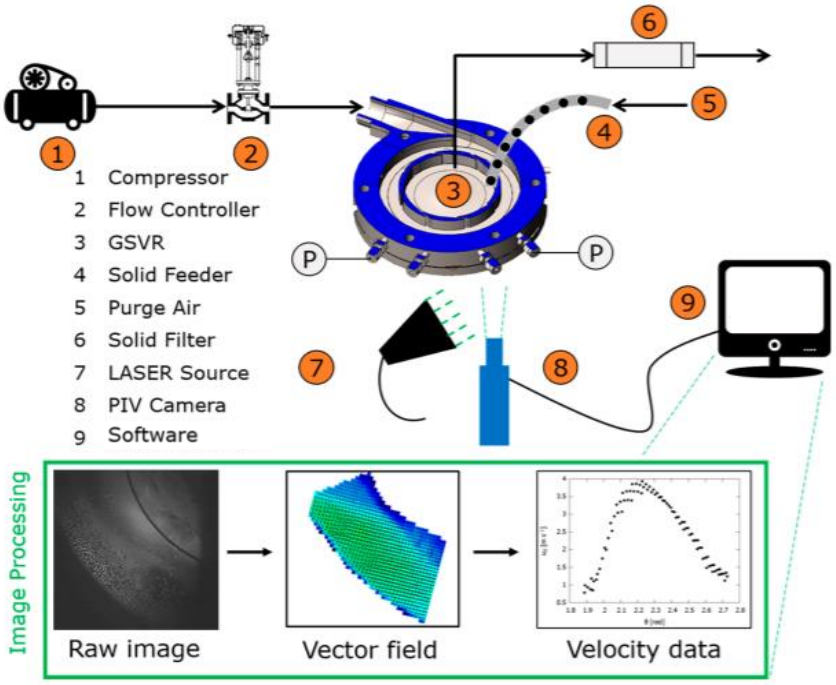

Figure 3. Overview of the PIV procedure in a GSVR setup[25].

If the goal is to analyze the fluid phase, tracers should be placed in the chamber. Those particles should be small enough to faithfully follow the dynamics of the fluid and big enough to scatter enough light to the sensor[26]. Hence, the velocity field achieved for the particles can be extrapolated for the fluid. If the solid phase is the one to study, those particles can act as tracers, since they can scatter light. Hence, this method can also be used to characterize the velocity field of the solids. The only requirement is that the particles from the solid phase can act as tracers[27].

One of the main advantages of such procedure is the capacity of analyze a wider area instead of a single point, as happens with the Laser Doppler Velocimetry[28]. For being also a non-intrusive technique, PIV can be applied in high speed flows or in boundary layers[22]. Therefore, it allows a great quantity large quantity of information that can be recorded instantaneously and simultaneously, being this the biggest advantage of such method[28].

Perhaps the biggest disadvantage of PIV is the possibility of decreasing the size of the tracers by the laser. Such diminishment will alter the results in two possible ways – improve their quality, since smaller particles will describe more truthfully the flow pattern or worsen it because smaller particles will

scatter less radiation, which will influence negatively the quality of the pictures taken. Either way, the results will be jeopardized and therefore not trustable[22].

Besides the presented features that can be achieved using PIV in the context of rotating fluidized beds, PIV can also offer information about the centrifugal force which is applied in a certain moment, in a certain point of the reactor. Velocity is composed by three components: radial, axial and azimuthal. In this context, the azimuthal component is the most relevant one, since it is in this one where the centrifugal force is expressed. Using PIV, one can know the value of such component and therefore calculate the centrifugal force in a certain point of the reactor – equation 2[13].

$$F_c = \frac{W_{s,max}}{I_N} \frac{v_{s,\theta}^2}{r} \quad (2)$$

Where $W_{s,max}$ is the maximum solid mass loading, I_N is the number of slots, $v_{s,\theta}$ is the azimuthal solid velocity and r is the radial position inside the chamber.

In the scope of this thesis, this technique will be depicted by the point of view of a multi-phase system. In a GSVR, gas and solid phases are presented inside if the chamber at the same time. Hence, PIV is used to monitor the behavior of the rotating bed. Therefore, the velocity and the arrangement of the solids in the bed is the characteristic to be studied.

Another technique that can be used to describe the flow pattern in a GSVR is Planar Laser Induced Fluorescence (PLIF). PLIF is an optical diagnostic technique widely used for flow visualization and quantitative measurements. Its principal is the fluorescence of the medium when illuminated by a source of light, usually a laser. The resulting signal is then detected by a sensor. That signal can be related with other properties and therefore allows to monitor those properties amongst the medium[29]. Such technique is also non-intrusive but can provide even more information about the fluid. Using such method, it becomes possible to measure the concentration of the present species, the temperature and the pressure of the system. Such properties are all designated as passive scalar properties, since they do not influence the physical fluid properties[30]. Thus, the combination of both techniques (PIV and PLIF) can provide a complete look over systems where fluid dynamics is important, since using both gives the operator information about the concentration of the present species and the flow velocity field.

In the work of Liu et al.[30], this technique is used to study turbulent swirling flow, such as the one observed in a GSVR, in a multi inlet vortex reactors (MIVR). The production of functional nanoparticles by flash-nanoprecipitation can be performed in a Multi-Inlet Vortex Reactor (MIVR). To monitor such process, a characterization of the velocity field can be done using Stereoscopic Particle Image Velocimetry (SPIV). This technique differs from PIV mainly because it uses two cameras instead of only one, giving therefore an in-depth perception of the medium. The two remaining components of velocity can also be evaluated when SPIV is used. This technology proved to be useful in this study since allowed to understand the importance of the axial component in such systems[31].

With such technique, the authors could identify two regions where mixing patterns were different. In the free-vortex region, the mixing structure was a spiral motion, whereas in the forced-vortex region it was nearly homogeneous. The phenomena that control the mixing in both regions was also

different. In the first region, mixing was controlled by turbulent diffusion and large-scale flow structures. In the second region, it was only turbulent diffusion the phenomenon which is responsible for mixing[30].

The combination of both techniques and some derivations are used by this group in several types of reactors, which results are published in the literature.

The turbulent mixing in a planar jet reactor was analyzed using PIV and PLIF, which provided concentration and velocity fields. The measurements were done in six positions where the turbulent flow was confirmed by the Reynolds number. CFD (Computational Fluid Dynamics) simulations were also done and both results were compared and showed to be similar. Such studies are important since turbulent flow provides best heat, mass and momentum transfer than laminar flow[32].

Temperature and Pressure Sensors

The operating temperature and pressure are perhaps two of the most important indicators of the state of a system. Both should be carefully controlled in any setup and a GSVR is not an exception.

For that purpose, both pressure and temperature sensors are usually installed in strategic places, such as the inlet, the bed and the outlet of the reactor. For identifying important locations where sensors need to be installed, use of CFD simulations is often made. For measuring pressure, two types of sensors can be used, differential and absolute. The absolute sensor is often used as a reference for the differential ones. Hence, measurements and recording of the pressure drop are possible between various sections of the reactor/unit. To monitor gas-phase temperatures, primarily thermocouples are installed in the chamber, in various positions, determined a priory. Using this methodology, a radial pressure profile of a GSVR was done and reported in the literature[33]. This study is done for two different systems – gas and solid phase and only gas phase. The pressure measurements are used to calculate the pressure drop of the system and to achieve a relation between the radial position and the gauge pressure of several locations of the reactor. Thermocouples are preferred as they are cheap and demonstrate quick response to changes in the temperature. Solids temperature measurement although is not easy and will be discussed in detail during the following section.

Heat Transfer in Vortex Devices

The rate of heating or cooling of a medium is crucial since monitoring the thermal behavior can provide great information about the subject. This issue gains relevance in a GSVR, since elevated heat transfer coefficients are a crucial characteristic of such technology and one of the main reasons why it is studied and used. Based on numerical Computational Fluid Dynamics studies, a rise in the gas to solid convective heat transfer, as compared to the conventional fluidized bed technologies has been confirmed[25,34]. The increased gas-solid slip velocity in the GSVR is at the origin of this phenomenon. Despite of this, experimental studies focusing on heat transfer are not commonly found in vortex literature. One of the reasons being difficulty in measuring solid temperature accurately.

An accurate measurement of solid' temperature in multiphase flow systems is complicated and not straightforward. Constant renewal of measuring point due to solid movement poses the first major hurdle. Depending on the operating conditions, solid velocities can vary between 0.5 – 10 $m.s^{-1}$ in the

device. Thermocouples, which are the most preferred, and cost-effective temperature sensors, tend to have a response time (of the order of few millisecond) much slower than the solid surface renewal speed (which is in turn proportional to solid velocity). The latter brings an inherent lag in temperature readings which is, of course, not desired for most of the applications. Secondly, thermocouples fall under the category of contact-type sensors. Consequently, thermocouples need to protrude into the flow field for an accurate particle temperature recording. This physical intrusion of a metallic wire provides an obstacle in the flow; significant enough to alter the local flow for turbulent conditions as seen in a vortex device. For particles with low Biot Number, the particle surface temperature differs from the particle internal temperature. Hence, for the reasons discussed, measurement with thermocouples can be misleading, especially for modeling purposes.

A solution to the above mentioned shortcomings of thermocouples could be overcome by moving to non-intrusive techniques, one of which being an Infrared (IR) Camera. An IR camera detects and measures the unique heat signature from a material (in this case, solid particles) by courtesy of a grid of sensors. The infrared energy that is received is converted into an image mapping the temperature of the object at hand. Each pixel in the camera sensor array converts the infrared energy focused on it into an electronic signal. The camera processor further converts the digital signal from each pixel, by using a mathematical transformation, to generate a temperature map of the object.

2.1.4. Applications

The applications of centrifugal fluidized beds are broadly documented in the literature. The uses for this technology, at least in a small and pilot scale, are very wide. A research made through the available literature is resumed in the next pages. Applications in various fields are documented, such as the food industry, fuel production, and biomass processing.

The study of the kinetic and potential energies of a system and their interaction, namely in systems of geophysical flows, like glass beads flowing down an inclined plane, under a centrifugal field were investigated[35]. The influence of the angle in the rotating velocity and in the height of the bed was described by qualitative relations. For higher angles and accelerations, larger velocities were achieved, in a proportional relation. For the same conditions, the height of the bed tends to decrease until a certain value, that is kept constant for larger angles or larger accelerations. The scaling up of such systems is also considered since a direct correlation between the velocities of the model and the prototype is documented. That correlation is based on the centrifugal forces acting on the system. Such correlation can help to diffuse centrifugal fluidization into an industrial environment, since there is a lack of knowledge in how to scale up rotating fluidized units, mainly because of its moving parts[35].

New approaches for the drying fundamentals in kilns and desorbers are also explored in rotating fluidized beds. Since the main mechanism of heat transfer is wall-to-bed, an analytical model to predict the heat transfer rate under such conditions was developed. The main innovation is that the proposed equation accounts for the effects of moisture evaporation within the bed, bed motion commonly encountered in rotary desorbers and time-varying wall temperature. By using the developed model,

more accurate results can be predicted for such systems, which mitigates uncertainties related to the time necessary to the drying process[36].

The production of catalysts is a complex industry, which accounts for a number of operations until the catalyst achieves its final form. At a certain stage, heating or cooling is mandatory to enable drying and then shaping the powder to its final form. For that purpose, calciners or kilns are used which work under centrifugal forces, whether they are generated by a rotating device or a vortex-like bed. Therefore, the study of the heat transfer in such devices is crucial for optimization reasons. With an accurate model to describe heat transfer during calcination and drying, the time spent in those tasks can be optimized, making the process shorter. Just like catalysts, there are other materials that need to be dried in a granular form during its industrial processing, namely coal, plastic pellets, metal ores, and fertilizers, just like described in the literature[37].

Rotating drums are largely used in the industry and they are constantly being optimized for industrial purposes. This equipment can process solids with a wide size distribution, has the capacity to process large feeding flows and solids with diverse properties are also not an issue for this device. Hence, scaling relations based on the equations that rule solid motion under such conditions are studied in the literature[26]. However, these relations are only applicable to certain ranges of particle diameter and temperature. For example, the model figuring this article is not applicable to particle diameters smaller than 100 μm, which fall in the range of Geldart A and C-type particles. As mentioned before, these are the particles on which a considerable part of this thesis is focused. Despite its limitations, such works help keep rotating drums updated to the needs of an increasingly demanding industry.

The food industry also takes advantage of rotating vessels, namely to dry food goods using air, for example an experimental study regarding the drying of chilies in a rotating fluidized bed device[6]. During each trial, the rotating velocity of the gas phase was kept constant as well as the temperature. Parameters such as the moisture, capsaicin (the active component of pepper) content and the color of each chili were evaluated. To achieve similar final moisture content, the drying time using rotating fluidized bed is in the range of hours, while days or even weeks are needed if the chilies are dried through sunlight. Controlling the capsaicin content of the chilies proved to be an easier task when the rotating equipment was used. Hence, using the rotating fluidized bed technique makes the process easier to be controlled and presents much better results when compared to natural drying, such as less during time and a lower operational temperature

The fuel industry has also seen this technology applied in hydrogen production. Feeding natural gas into a vortex flow reactor and exposing it to the sunlight leads to a carbon and hydrogen generation (the ruling reaction is $CH_4 \rightarrow C + 2H_2$). The radiation from the sunlight decomposes the methane molecules in carbon and hydrogen, along with the consumption of energy, since this reaction is endothermic. By this path, the carbon formed is of nano-filamentary nature. This process shows many advantages when compared with the most used, which consists of burning natural gas. Since there is no flame or burning of any kind, there are no oxides formed. Therefore, the carbon obtained is free of impurities. Another consequence of not having a burning process is that there is no CO_2 emitted to the atmosphere, and therefore decreasing the amount of pollutants associated with the process. Lastly, the

solar-driven process upgrades the calorific value of the feedstock by adding solar energy in an amount equal to the enthalpy change of the reaction. It also offers the possibility of storing and transporting solar energy[8].

The application of protective coatings in solid particles is a process that also fits the characteristics of centrifugal fluidization units. Once the bed is fluidized, coatings are sprayed from several angles to the particles. A protective layer will be formed in the surface of those particles. Most of the times, that layer protects the particle from the surrounding environment or from sunlight. The mixture that is sprayed is often achieved mixing a solvent with the material with coating properties. After the spraying, the particles are dried using air, so the solvent can be evaporated[38].

The SO_2 and NO_x adsorption process – SNAP – from flue gases with an Al_2O_3-based sorbent is a process by which pollutants can be sequestered from gas streams which would end up in the atmosphere. It's a treatment process which suffers significant improvements when performed in centrifugal units since this technique provides very small gas-phase residence times and a large volume throughput[39]. Therefore, intensification is achieved in two aspects: much larger slip velocities and higher interfacial mass transfer. The main disadvantage of the process is the pressure drop, which can be 20 times higher than in a riser[4].

The principal of vortex reactors was also adapted to a different geometry – the torbed reactor. In this reactor, the gas phase is fed from the below of the plate (in a vertical axis configuration of the reactor), where several blades are arranged with a specific angle. Passing through those blades, the gas phase pattern flow is changed, and it starts rotating around a central cone disposed of in the middle of the plate, as show in Figure 4. The solid phase is fed from the top, slides along the cone and forms a bed on the top of the plate. As in a vortex reactor, all parts are static in this reactor as well [40].

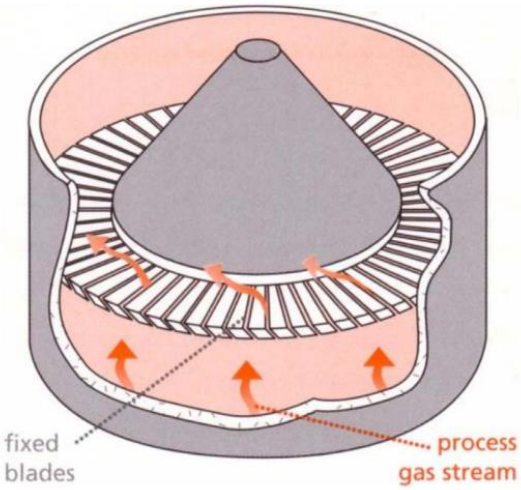

Figure 4. Torbed reactor[41]

The main difference between torbed and vortex reactors is the geometry of the solids feeding system. The distribution of the solid phase is much more uniform in the torbed reactor than in the vortex one since the particles are distributed around the cone, while in the vortex geometry the solids are

usually fed in a single radial position. The main disadvantage when this technology is compared with the vortex one is the impossibility of removing the particles while operating the unit, what can be done in vortex reactors though not in a continuous regime.

The applications of such technology are linked with mineral processing, toxic waste destruction, pasteurization, and materials recycling[40].

2.1.5. Centrifugal Dryers

Centrifugal dryers are a huge application of centrifugal fluidization and largely documented in the literature. The drying process can be applied to porous particles or for superficial drying in non-porous particles. Many drying processes are present in the literature, including food goods, amorphous materials, and biomass.

The drying of non-porous particles[42] is one of the examples. The materials used are glass beads and wet sand. The operation occurs in a centrifugal fluidized bed dryer, with a rotating geometry. The changing parameters were the bed height, the centrifugal force, and the Reynolds number. From those trials, a model to heat transfer was generated. The article also explores other types of materials, namely slices and blocks of potato, which have a larger porosity than the ones mentioned before. Although these differences, the influence of the porosity is never mentioned. A lack of information on how particles with different porosities behave under the conditions of a centrifugal dryer is noticed. Regarding the different shapes of potato, is concluded that the optimum dimensions for each material should be determined for a set of operating conditions.

An experimental comparison between the drying of biomass under gravitational and centrifugal forces is also present in the litearture[9]. To compare the performance of both systems, a process intensification factor is established. It is defined as the ratio between a certain variable obtained for the centrifugal fluidized bed with a static geometry and the gravitational bed. Using the centrifugal technology and in terms of the specific drying rate, it was possible to intensify the process by one order of magnitude. The stage of drying that has seen more improvements was the first one, the constant rate period, where the vapor pressure in the particle surface is equal to the saturation point of the surface temperature.

There are 3 characteristics that make centrifugal fluidization more powerful: the higher gas-solid slip velocities, which leads to higher interfacial heat transfer coefficients; a denser and a more uniform bed. From these three, the most significant one is the density of the bed. In a centrifugal bed, the bulk density of the bed is much higher than in a gravitational one. On the other hand, the slip velocities do suffer an increase but it's not substantial. All these improvements come with the cost of higher air consumption, which is six times higher than the amount needed in a gravitational bed. Nevertheless, air usage efficiency is maintained. To diminish the consumption of air, recycling can be considered, as long as the moisture content is far from reaching the saturation point. During operation, it was noticed that the moisture content of the particles inside of the reactor was lower than the particles in the outlet region.

The cause is a partial bypass of the biomass. This issue can be solved optimizing the feeding and the outlet geometry of the solids, making it similar to the one used for the gas phase, which implies getting several inlets for the solids distributed over the chamber.

Once more, scaling up can be an issue, mainly related to the non-uniformity of the results and the consumption and usage of the gas phase[19]. Some suggestions are made to improve those issues, like working with several zones inside the same chamber, which replicates the behavior of a battery of CSTR'S. To decrease the amount of air used the presented solution is to make it flow through several chambers. A single use represents a waste of potential since under these conditions, the air rarely reaches its saturation point. A different behavior of bubbles and mixing regimes for different bed sizes were also verified[3]. In smaller beds, the solid phase is dragged along with the gas phase, whereas in larger beds there is recirculation near the walls. Remark that the size of the bubbles in both cases is similar. It's the flow patterns that change that may differ from bed to bed. Therefore, this group is skeptical about results obtained in a laboratory scale or even a pilot scale, since most of the changes that the system can suffer will not be predictable in those environments. None of those can assure the fluidization will work on an industrial scale.

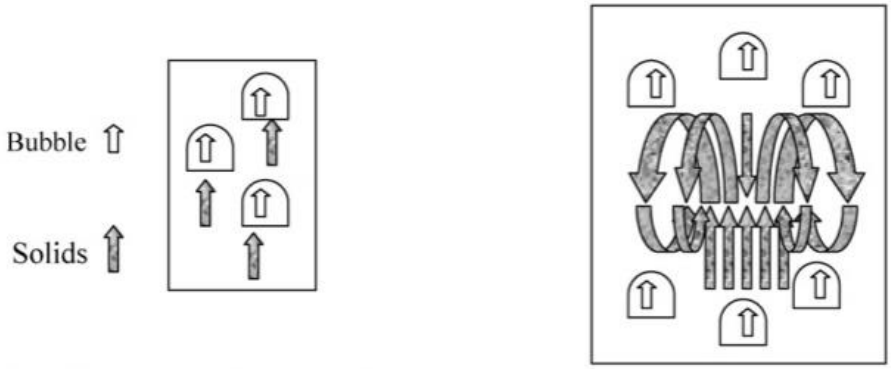

Figure 5. Flow patterns in beds with different sizes.[3]

2.1.6. Particle Segregation

The segregation of particles by their size and density is a promising feature of GSVR's which still needs to be explored. This advantage can be applied in processes during which the particles suffer a decrease of size or density or new ones are formed during the ongoing process. Those changes can be caused by a reactive or non-reactive environment.

The interesting feature of segregation which can be applied in a GSVR is the change of radial position inside the reactor depending on the size or density of the particle. When a particle becomes smaller/lighter, it will travel radially inwards inside of the reactor and therefore it will be easily entrained from the chamber. If a particle loses mass, either because diameter or density changes, the centrifugal force applied will decrease and therefore its radial position in the chamber will change. A wide distribution of the particle sizes in the bed is linked with segregation since the forces acting on each particle have different impacts. The forces acting on the system are the same but their impact on each particle it's not[43].

One application of this feature would be chemical looping combustion (CLC) of coal. In CLC, a typically metallic oxygen carrier is transported between an air reactor where the oxidation of the carrier takes place and a fuel reactor in which combustion of a hydrocarbon proceeds with the oxygen provided through the oxidized carrier[10]. The GSVR technology shows potential for the second part of the process, specifically to separate the carrier from coal and from ash. Using a centrifugal unit like GSVR would provide in-situ separation in a single unit operation. Using the GSVR technology for CLC would decrease the costs related to equipment and operation and would intensify the process.

A few theoretical studies, using CFD simulations, were done on the topic and described in the vortex literature[10]. The flow pattern of a system constituted by air and a mixture of two different solids in a GSVR was simulated in order to study the separation of phases and particle segregation. That mixture was composed by two different materials: type 1 – big/heavy particles (1mm and 2700 $kg.m^{-3}$; 4.864 $kg.s^{-1}$) and type 2 – small/light particles (0.4 mm and 200 $kg.m^{-3}$; 0.032 $kg.s^{-1}$). The main gas used was air. A standard solids' inlet design was implemented.

Although the simulation time is only 1 second, three stages of the system were studied. In the first 0.1 seconds, only the gas phase was fed into the reactor. The formation and stabilization of the free vortex happened during this stage. This proved to be a very strong vortex, occupying the entire chamber. The highest velocities (above 35 $m.s^{-1}$) are detected in the free board region.

Once the solid mixture is fed to the reactor, the free vortex loses strength. From this moment on, it is possible to see different flow patterns for each type of particle. The small/light particles present a higher rotation velocity when compared with the larger/heavy ones. Therefore, only 0.25 seconds after the beginning of the second stage, some of the smaller particles have already completed one rotation. The particles are mostly found close to the wall. As the feeding continues, particles with different properties assume different radial positions, but that arrangement is not clear enough to distinguish two different beds. Another phenomenon worth to be mentioned is the loss of both types of particles through the chimney, in an early stage of the simulation. This happens almost from the beginning of the feeding. There are two possible explanations: bypassing, which is also mentioned in the literature[9], of the fed solids, causing an early entrainment of the solid phase; or the collision between the incoming particles and the ones which are already rotating inside the chamber. This last reason would lead to the disturbance of the bed, and, once more, to an early entrainment of some of the particles.

In the last stage, the effect of feeding in the bed stability was evaluated. Without particles entering the reactor, the freeboard region is free from solids. Therefore, the free vortex presents itself stronger. Alongside with this effect, phase separation and particle segregation gain importance. The formation of two beds happens in the chamber. One closer to the circumferential walls, denser, where the heavier particles stay and one closer to the free board region, less dense, where the smaller particles are rotating. Because of its lower density, this second bed can assume a vortex free-like behavior. In both beds, it's possible to find a small percentage of particles from the other type. When small particles are found amongst bigger ones, they get trapped in the voids and are not likely to leave. When the opposite happens, the big particles easily leave that radial position, travelling outwards in the chamber to the periphery.

From the above analysis, the authors propose the creation of outlets for each type of solids, using the chimney only for the exit of the gas phase. The optimization of the solids' inlet is also suggested, since it can be the reason of unnecessary losses and disturbance in the rotating bed. This work does not present any experimental validation and the reason why the inner bed is less dense than the outer one is not clear, since the mass of smaller particles is so small compared with the amount of bigger particles fed.

Within the same subject, the influence of small/light particle size and density in the rate and quality of particle segregation in a GSVR was studied through CFD simulations[44]. The study concludes that keeping the properties of the big/heavy particles constant, the segregation observed is fast and efficient for a large range of sizes and densities of the small/light particles. It is also concluded that a faster or more pronounced segregation is obtained when the particle diameter or density ratio are increased. An optimal particle diameter ratio is also found. Above that value, the edges of the beds become irregular and contamination with different particles happen. Below that value, the difference between diameters is not big enough to form two distinctive beds. This study strives to combine the effects of particle segregation, gas-solid contact and gas-solid separation, which are all enhanced by a high-G field. The scope of the article is a step closer to be achieved, since a range of successful operating conditions is attained.

In a more practical approach, particle segregation is studied experimentally in a GSVR, when integrated in the above-mentioned CLC of coal[45]. For this purpose, a GSVR is used to separate a mixture of granular materials inside of the chamber from the oxygen carrier, which is successfully achieved. Since the mixture is formed by particles with different sizes and densities, the formation of two distinguish beds is observed. Other systems are experimentally studied, including cork, glass beads and high density polyethylene (HDPE). In the case where glass beads and HDPE are fed to the reactor, no segregation is achieved, since low drag and centrifugal force are associated to glass beads, in opposite to HDPE, which particles are under high drag and centrifugal force.

The principle of segregation is still a concept that needs development and a more accurate theoretical and experimental understanding since the literature lacks information about the subject.

2.1.7. Process Intensification

Process intensification (PI) is a topic which received much attention by the industry world since aiming for improvements in industrial processes is a growing need. The aim for greener processes is also a reason for which process intensification gain so much attention lately. Demanding policies in what concerns industrial processes has increased the interest in the process which can be developed in smaller, less pollutant and more efficient setups.

Using the definition proposed by Stankiewicz and Moulijn, PI is '*Any development that leads to a substantially smaller, cleaner, safer, and more energy efficient technology*.'. The level of improvement that is expected when a process is submitted to intensification must be considerably high since the

modifications done imply questioning and adapting processes that were used for decades. Therefore, the changes should be such that the results are hundreds of percent better compared with the ones obtained before.

To do an accurate and successful PI analysis to a process, some steps are suggested [46]. The process driving forces should be identified and an overview of the process should be considered. These first steps allow evaluating the weak spots of the studied procedure. The rate-limiting steps are also an important feature which should be carefully investigated. After this first approach, an attempt to generate new design concepts and analyze design alternatives should be done, to improve the weaknesses found before. For the found solution, a suitable equipment should be chosen or adapted from an existing one, if required. The final step is to perform the process in both setups and by means of a process intensification factor, compare the obtained results and decide on implementing the intensified process.

Process intensification can still be applicable for two different subjects: process intensifying equipment and methods[46]. The first one strives to improve critical operational parameters, mostly related to the driving force of each procedure. The second one focusses on the integration of several processes in one equipment.

The vortex technology is an example of process intensifying equipment since the heat and mass transfer coefficients are largely improved when this equipment is used. Such variables are related to the driving force of processes like drying, one of the main applications of GSVRs. Those improvements are mainly due to mechanical changes. The reactor geometry (the feeding of the gas phase and the chamber itself) leads to centrifugal fluidization, which will enable higher mass and heat transfer, improving the chemical variables of the process, such as the yield of the process or the drying time. Besides, the size of the unit can be quite small when compared to gravitational technologies, since the residence times of both phases are considerably smaller under centrifugal forces. Other aspects, such as segregation based on particle diameter or density, which will be studied in this work, can perhaps replace or diminish the need for separation devices downstream. If the segregation of particles is proven to be a successful and feasible way to separate particles, the GSVR can also be included in the category of process intensifying methods.

Regarding solids handling, the literature points to several directions. The use of hybrid technologies which allow to combining operations or processes into single equipment to minimize the unit operation size, lower the energy use and cost and reduce the operation time is one of them. Using alternative energy sources as a magnetic field, microwaves or ultrasound are being studied but they will not be loomed since they are not part of the scope of the present work. Lastly, anti-fouling techniques are being considered, since PI is close-banded with miniaturization which in an extreme point will lead to problems related to fouling and blockage. Surface modifying and dynamically changeable structures seem to be promising technologies[47].

2.1.8. Conclusion

Once the nowadays context of the GSVR was explained, new challenges emerge. The potential of the presented technology is so vast, yet there are many questions waiting for an answer regarding some unexplored nuances of such equipment. What is the true potential of segregation? In what extend the vortex technology can overcome the difficulties of fluidizing small particles? What fluidization behavior should be expected once a particle is fluidized under centrifugal forces? The next chapters strive to provide an answer to these questions.

2.2. Fluidization of Geldart A and C-type particles – a challenge yet to be overcome

As stated in the work of Geldart[48], the fluidization of A- and C-type particles are the most challenging ones. In the Geldart classification, presented in Figure 6, these are the groups with lower particles sizes (less than a 100 µm) and lower densities (typically under 1500 kg.m^{-3}).

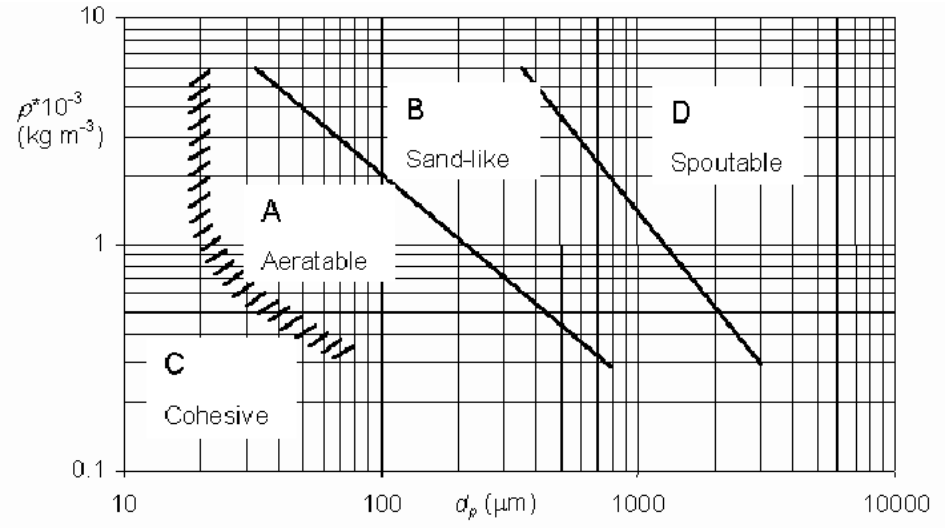

Figure 6. Geldart classification for gas fluidization[48]

Belonging to these, there are several materials which applications are related to fluidization and solid-gas phase systems. The ZSM-5 zeolite is an example of a Geldart A-type particle which is widely used in the petroleum industry in heterogeneous operations, namely in hydrocarbon isomerization reactions[49]. Calcium carbonate in the form of limestone is a Geldart C-type particle which is commonly used in the chemical industry. Its applications fall in the range of the paper industry, in coatings for paper and paints and to refined sugar, namely for removing colloidal impurities. Outside the chemical world, the limestone is also used to manufacturing construction materials and cement.[50]

According to the properties of the particle, a different fluidization behaviour will be observed. In respect of the C-type particles, the interparticle forces intrinsic of those powders, namely the Van der Waals forces and electrostatic, are stronger than the force that the gas phase can impart on those

particles, causing plugs in smaller diameter beds and channelling in larger beds. The fluidization state is difficult to achieve for particles belonging to this group because of interparticle forces. Therefore, these particles are characterized as cohesive.

Some of the mentioned difficulties in fluidizing Geldart C-type particles can be overcome using external means, such as vibration, rotation, centrifugation or a magnetic, electric or acoustic field[3,20]. Developments regarding improving the fluidization of cohesive particles are presented in the literature as coating techniques. The surface of the bigger particles (or host particles) is covered with nanoparticles (guest particles), decreasing the interparticle interactions and therefore diminishing the cohesive effects. This process is called functionalization and its applications are very broad. It can be used to modify the flowability, dispersibility, fluidization purposes, homogeneity of the surface, content uniformity and dissolution profile[51]. By using this method, the intrinsic properties of the particles are being altered, namely the surface characteristics. Another method to improve the fluidization quality of cohesive powders is to mix those with particles having different size or shape[20].

Concerning the particles which dwell in A type, the bed will expand considerably before bubbling starts, but fluidization is hardly achieved under gravitational fields[48]. Phenomena as slugging and channeling are also common in such operations[4]. A bed formed by particles which properties match the A-type is classified as aeratable since the gas phase can pass through the bed, but the flow pattern cannot develop enough to attain fluidization.

The fluidization of Geldart A-type particles under gravitational forces was numerically studied[52] and the influence of each pair of forces present in the system was correlated with their fluidization behavior. Through simulations, this study concluded that the bubbling regime is mainly caused by fluid-particle interaction, which is the dominant pair of forces. Moreover, during homogeneous fluidization, there is no main effect since this stage is described as a transition period while the three pairs (particle-particle, which includes particle-wall interaction; gas-particle and interparticle forces, such as Van der Waals forces) act at the same extent, which results in competition and absence of a pronounced effect. Usually, this stage is classified as unstable, since the interactions between the fluid and the particle are very strong. Consequently, the velocity of the particles increases, destabilizing the bed. Since the other two pairs of forces have several directional components, and if each component is significant enough, the bed can be stabilized increasing one or both. The challenge is to lead the system to a homogeneous fluidization stage and to keep it there, maximizing the heat and mass transfer coefficients.

However, there are other theories related to the homogenous fluidization of Geldart A-type particles under gravitational forces in literature. The previous theory stated that for this regime there is not a demarked effect from any of the pairs. Two hypotheses are evaluated related to which pair has more influence under this regime, if the fluid-particle or the particle-particle pair. The discussion has relevance since both theories are sustained by experiments but not in a satisfactory way, as both present flaws. Two important aspects about the fluidization of these particles are the minimum velocity of bubbling, defined as the gas phase velocity when the first obvious bubble appears, and the minimum velocity of fluidization. For the first-mentioned parameter, the influence of Van der Waals forces is almost null. Otherwise, this type of force has much more influence on the minimum bubbling velocity. Increasing

those forces will lead to an increase in the minimum velocity. If that increase is substantial, the fluidization behavior will change, shifting for typical C-type comportment.[53]

Bearing in mind the advantages present before in this work related the centrifugal fluidization, is expectable that the fluidization of Geldart A-type particles would be reached easily. A search among the available literature was done and one article was found. Although there are several articles regarding the fluidization of ultrafine particles (nanometer scale) for coating purposes, none of them mentions the use of Geldart A-type particles.

The fluidization of glass beads with a diameter of 100 μm in a rotational fluidized bed is described in the literature [54]. The particle density is not provided, but with such diameter, these particles most likely belong to group A from the Geldart classification. Therefore, under gravitational forces, these particles are expected to form a bed which will suffer a considerable expansion before fluidization, if this stage is achieved at all. Agglomeration is also verified during the reported experiments. When the particles are submitted to centrifugal forces, specifically 16G, its behavior changes. The bed also expands but the fluidization stage was easily achieved, and the surface of the bed was irregular. Introducing carbon particles in the chamber and the gas phase, mixing between both particles was verified. This happened without agglomeration of the glass beads or distinguish bubbling formation. The pressure drop of the glass beads under 9, 16 and 37 G was evaluated. For the first two scenarios, this parameter assumed the same behavior as in gravitational systems, increasing linearly with the gas phase velocity and stabilizing at the minimum fluidization velocity. For the highest centrifugal force, that limit was not reached. Estimations of the pressure drop vs. gas phase velocity where done which considered particle entrainment and bed expansion. The experimental data was clearly similar to those estimations. Later, the results published will be compared with the ones achieved in LCT for the present work.

The influence of coating cornstarch (a group C powder, according to the Geldart classification) with an aqueous solution of hydroxypropylcellulose (HPC-L) in the cohesive properties of those particles was evaluated. The procedure took place in a rotating fluidized bed coater. By the end of the process, the particles presented a much more uniform surface which implies that the bed was successfully fluidized. The releasing time of the drug was extended without compromising the agglomeration state of the particles. Besides, an effective way for fine particle coating of cohesive fine powders was also found.[18]

Some of the presented examples use coating as an improvement tool for the cohesive properties and others' purpose is to modify its surface properties without jeopardizing the initial agglomeration state.

The effect of mixing ultra-fine particles (Geldart C-type) with fine particles (Geldart A-type) is studied[43]. By mixing such particles, a simulation of the effects of breakage or surface abrasion of the fine particles is aimed. This scenario would drastically change the particle size distribution and the fluidization behavior of the bed under gravitational forces. There were several mixings studied: 30, 50 and 68% (w/w) of ultra-fine particles. Increasing the percentage of ultra-fine particles delays the starting

of partial fluidization, which was the only type of fluidization achieved, and increases the bed pressure drop. Having such a wide size distribution leads to small void sizes, a greater air retention capacity, enhanced fluidity and partial mixing of the particles. The properties, such as the bulk solid flowability and the bulk density, of mixtures with higher content of ultra-fines are similar to the properties of those ultra-fines isolated, e.g. not mixed with anything else. Hence, smaller particles have a large effect on the properties of the bed and consequently in the presented fluidization behavior. The researchers also state that the reproducibility of these experiments is null since the fluidization behavior presented in each trial varies between cracking, channeling, and agglomeration. Therefore, a pattern is not possible to establish. To conclude, there are several effects in mixtures between ultra-fine and fine particles which are not clear and strive for more investigation. Although, such effects improve the quality of fluidization of ultra-fine particles for two reasons – agglomeration between particles with a different size and the separation of the previously formed agglomerates, caused by friction and collisions. The breakage of these agglomerates creates smaller agglomerates but improves the size distribution, which enhances the fluidization. Agglomeration is important because bigger 'particles' are formed, with higher kinetic energy and higher density. The conclusions from this article cannot be directly applied to centrifugal fluidization since other parameters arise. Although, it is expected that the effects observed by mixing fines and ultra-fines can be enhanced under a centrifugal field.

2.2.1. Conclusion

Concluding, the fluidization of small powders is getting more attention from the researchers, mainly under centrifugal forces, since using a classical gravitational fluidized bed has proven to be difficult. There are a few techniques used to ease the process reported in the literature, including functionalizing the particles, coating techniques, vibration, and other external means. The use of the vortex technology has proven its worth in improving the quality of the fluidization of such small particles, which is a good indicator for the work ahead, which consists in, first, successfully fluidized particles belonging to the mentioned groups and, secondly, study its behavior under centrifugal forces once they are fluidized. This subject will be discussed in the following chapter.

2.3. A Geldart-type chart for centrifugal fields

Geldart [48] presents a graphical way to classify gas fluidization behavior of powders, according to particle diameter and density. The resulting chart is influenced by many factors, such as temperature, pressure, gravitational forces, cohesion, air viscosity, the adsorption of the gas in the particle and gravitational acceleration.

The graph, presented in Figure 5, is divided into 4 groups – A, B, C and D. Each of them represents a different fluidization pattern. For particles belonging to group A, the bed suffers a considerable expansion before bubbling starts. Because of the expansion of the bed, these particles are classified as aeratable. For B-type particles, the bubbling starts at the minimum fluidization velocity. The bed expansion is small, and the bed collapses rapidly when the gas phase ceases. In the absence of

bubbling, the power circulation is little to non-existing at all. The main difference between these two groups consists of the degree of expansion observed. Higher expansion means the particles belong to group A, while little expansion indicates a group B material. In beds constituted by C group particles, slugging and channeling are two possible scenarios. For smaller beds, the powder tends to lift as a plug and for larger ones, channeling is recurrent. These particles can only be fluidized in an agglomeration form, which is not easily achieved because of the plug formation or channeling in the bed. Finally, particles fitting the properties of D group will probably form stable spouted beds [20,48].

When one chooses fluidization as the technique to deal with a solid-gas system, usually high mass and heat transfer coefficients are aimed. For maximizing those, bubbling should be minimized. Therefore, the quality of fluidization is often linked with such property. Following that thought, the quality of fluidizing Geldart A-type particles is better than Geldart C-type particles and so on [20].

2.3.1. Geldart Classification Under Centrifugal Field

During operation in GSVR's or any other kind of unit where a centrifugal field is present, the Geldart classification is not appropriate, since shifting between groups is reported in the literature[20]. Particles with density and diameter in agreement with group A showed a fluidization behavior closer to the one expected for group B. Therefore, a need to create a new Geldart-like chart that gathers the fluidization behavior for solids with different densities and sizes under centrifugal forces arises.

The work available in the literature compares the fluidization pattern achieved in a gravitational fluidized bed and a rotating fluidized bed[20]. Geldart C-type particles – 7 µm Alumina with a density of 1470 $kg.m^{-3}$ – were submitted to several centrifugal forces, between 7 and 278 G. For lower centrifugal forces, the particles present a typical Geldart C-type behavior, with agglomeration, a bed surface nonuniform and formation of channels among the bed. Increasing the rotating velocity (and therefore the centrifugal force), the channels diminish in size. At 34 G, the particles start to separate from one another, which represents a shifting in the fluidization behavior, since it is possible to fluidize the bed without solids agglomeration. Although this changes, it is still not possible to define the fluidization behavior as one single group. At 56 G, there are no agglomerations among the bed and the surface presents itself as uniform. Increasing, even more, the centrifugal force applied, the particles presented themselves as belonging to group A or B. Distinguish between these groups is difficult since the only difference is the moment which the bubbling starts, if before or at the minimum fluidization velocity. Because of this, the authors decided to create a A/B group, which is considered to be a stable state of fluidization.

This article obviously concludes that the fluidization behavior of the same particles shifts with the forces field applied. To stronger fields, e.g. centrifugal ones, the quality of the fluidization is better, and it's easily achieved. However, to reach such stronger fields, the usage of the gas phase reaches values that can be too high and therefore unfeasible the operation [20]. Other researchers also conclude that viscosity has the same effect on fluidization quality than increasing the acceleration field [55].

2.3.2. The evolution of the Geldart Classification

Other attempts at designing a Geldart-like chart were done and reported in the literature. Such tries were done focusing on and using different approaches, which will be reported in the next pages.

The Geldart classification as it was first presented does not apply in an industrial environment, since most processes are performed at higher temperatures and pressures and with other fluids rather than air, which modifies the fluidization behavior of the solid phase. Therefore, a re-interpretation of the Geldart classification based only on examples found in the literature is presented[56]. The authors present several situations in which the powders shift from one group to another under certain conditions, as is the case of Geldart B-type particles fluidized by supercritical carbon dioxide under high pressures. Those reasons are the motivation for their work.

This new classification, represented in Figure 7, which plots a dimensionless density $\left(\frac{\rho_p - \rho_f}{\rho_f}\right)$ against the Archimedes number, allows representing the same powder in different parts of the graph, but only if the density of the fluid is different. It also allows representing in the same plot powders with different properties, fluidized at different pressures and temperatures and by gases of different nature.

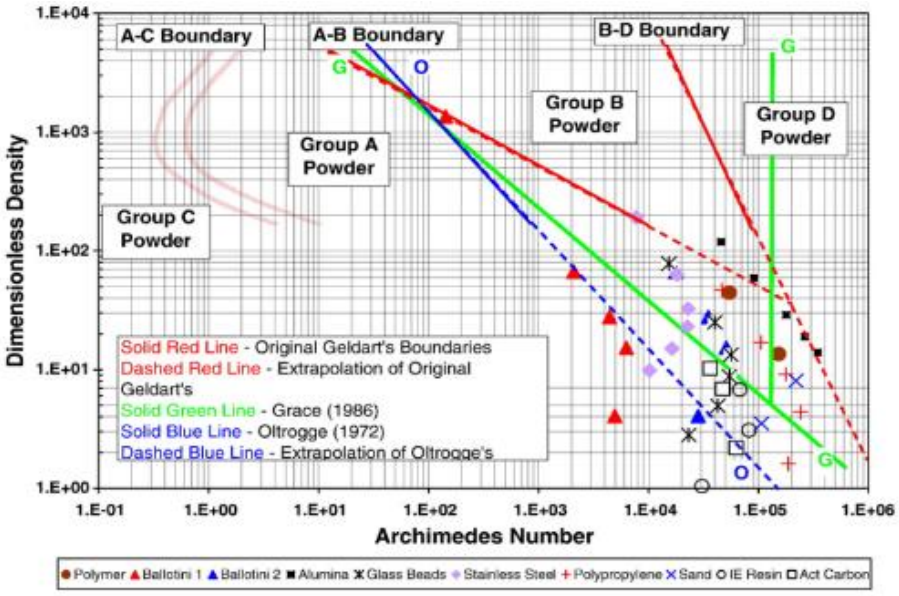

Figure 7. Graphical classification for gas fluidization of powders under industrial conditions[56]

Therefore, the range of situations where this classification is applicable is much higher than the one proposed by Geldart [48] and some heuristics can be assumed by analyzing this graph: increasing the fluid density and viscosity enhances a Group A-like behavior; the same happens for higher operating pressures. However, changing the temperature does not have a straightforward effect, since it leads to a decreasing fluid density and an increased fluid viscosity. Comparing the results given by the new classification with the ones reported in the literature, the results are remarkable. Hence, this new graphical classification of gas fluidization of powders appears to be very accurate. However,

experimental confirmation by the authors would add value to the work, since all the data presented was collected by themselves from the existing literature. Another aspect worth mentioning is that the result achieved can be unpractical if one chose to use in the everyday life.

Another aspect of the original classification of Geldart that was evaluated is the cohesive forces. On that first attempt, the cohesive forces considered between particles were only due to Van der Waals forces and electrostatics. However, if the powder is wet or contains a high amount of moisture, the cohesive forces will change, and most likely, become stronger. This situation was not predicted by Geldart and therefore the need to improve his original classification[57].

For that purpose, several solids with different moisture content were evaluated and changes in the fluidization behavior were detected. Two different systems of fluidization were used to study two different forces. A system where fluidization is performed with water and Geldart C-type particles and a second one, where air and Geldart D-type particles with high moisture content are studied. The focus on the first system is to study the Van der Waal's forces, which are weaker in liquid mediums. On the other hand, the second system will be used to study liquid bridges, which augment the cohesive forces. Both systems operate only under gravitational forces.

These two forces play an important role in particles which are commonly fluidized. The Van der Waals forces are present in particles which are 100 μm or less and are mostly due to charges interactions. The liquid bridges are formed when two particles present some moisture in the surface. This force augments the attraction between those two particles, making more difficult to separate them. Generally, in the presence of water, the liquid bridges are stronger than the Van der Waal forces. However, this situation can change according to the amount of moisture on the surface of the particle.

Analyzing the results from the experiments, a clear connection between the moisture content and the fluidization behavior is achieved. Geldart D-type particles which have a significant amount of moisture present a behavior close to the one expected for A or C solids. As predicted, the Van der Waals forces are weaker in aqueous mediums than in air mediums. Although these conclusions, a graphical classification is not provided by the researchers.

The last example presented in this section emphasizes the importance of nanoparticles for the industry, which is related to their appealing characteristics, namely high surface area, which is linked to higher mass and heat transfer coefficients and to better quality surface catalysts reactions and coating purposes. Although these solids are, in theory, and partially, included in the original Geldart classification, studies report that particles with such small diameters do not always present a C-type typical behavior[58].

Therefore, this study[58] evaluates the gravitational fluidization of zinc and copper oxide particles with 50 nm and a density of 5600 $kg.m^{-3}$. For such small particles and high velocities, a more accurate technique than eyesight is required. The chosen one is X-ray microtomography imaging, which allows the operator to observe the bed and its behavior without destroying the material and obtain real-time and *in-situ* information.

Particles with a diameter smaller than 50 µm, the surface forces begin to dominate, which leads to an increasing cohesiveness. Hence, agglomeration tends to happen. With bigger agglomerates, the short-range forces which are linked to cohesiveness get weak, changing, therefore, the fluidization behavior. Higher particles become more easily fluidized and hence many articles have been published[59-62] with the scope of fluidizing nanoparticles by the production of dynamically stable and large agglomerates. Those agglomerates can reach diameters of microns or even millimeter-order of magnitude. The agglomeration degree was studied with the X-ray microtomography imaging technique.

At small air velocities (0.052 $m.s^{-1}$), the agglomerates present a behavior close to the one expected for A and B particles. The bed is divided vertically into two regions. In the bottom, the bed is fixed, and channeling is often observed. On the top, bubbling and turbulent flow tends to happen. At higher air velocities (0.078 $m.s^{-1}$), the previously formed agglomerates break apart, but because of the cohesive forces, the small pieces become an agglomerate again. This process is called dynamic nanoparticle clusters.

Because of this dynamic, a new group of fluidization behavior was established. This group, designated as E, stands for 'expandable' and occupies the bottom part of the C group proposed by Geldart. The main reason to create a new group is the importance of the short-range forces and its influence in nanoparticles with a density smaller than 100 $kg.m^{-3}$. Remark that such small densities are associated with clusters and not to the nanoparticles itself.

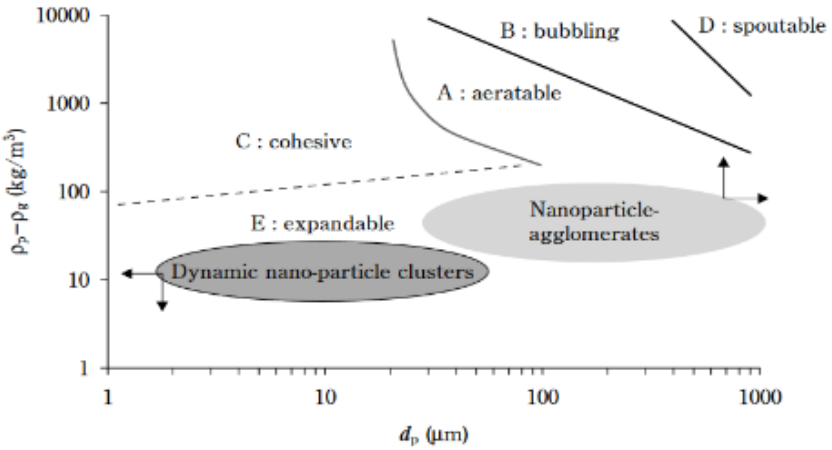

Figure 8. Proposed graphical classification for gas fluidization.[58]

With this work, a more complete classification of the types of gas fluidization was achieved. An advantage of the proposed graph is the ease in utilization, something that is not always a priority.

2.3.3. Conclusion

In short, many attempts to improve the Geldart classification were done over the years. Reasons of industrial nature are the motivation for many of those since the old classification could no longer respond to the needs of the industry. Some of the proposed classifications are easy to use than others

and some present a broad range of application. However, a paper reporting a classification for systems under centrifugal forces was not found in the available literature. The closer that was found to the meant scope was a comparison between the results obtained under gravitational and centrifugal conditions, which demonstrated not be sufficient for the industry to fully understand the gas fluidization behavior of particles under such circumstances. With the increase of the use of centrifugal fluidization, a clear need to adapt the Geldart classification to centrifugal fields arises. Remark that designing a graph applicable for general centrifugal forces it's not possible since these forces can assume several values and therefore imply different behaviors for the bed. Hence, a graph should be designed to a specific value of centrifugal force.

2.4. Final Considerations

With this literature review, a state of art about fluidization under centrifugal fields was provided, with particular focus in vortex technology. This has a huge potential and its use amongst the industry could be broader if more attention was brought to the subject. The need to comprehend phenomena such as segregation is mandatory to take this technology to an industrial-application level. New paths are opened by such devices, namely the fluidization of Geldart A- and C-type particles, which importance and use in the chemical industry is quickly growing. The development of pragmatical tools, that can be used in a daily basis, such as a graphical fluidization classification under centrifugal fields, would bring a first impression on the system and therefore, a quick understanding of the fluidization behavior that can be expected from a certain particle.

3. A Mathematical Model – Critical Particle Diameter

As explained in the previous chapters, the design aspects of a GSVR greatly influence the possible operating conditions associated with the unit. The swirl ratio and the dimensions of the unit cannot be easily changed during operation. For that reason, a GSVR has the disadvantage of narrowing the diversity of processed materials and operating conditions (e.g. the main gas flow rate). Hence, a necessity of understanding which materials can and cannot be successfully fluidized in a certain reactor arises. For that purpose, a mathematical model was constructed and presented in this section. Besides the presented objective of the model, it can also be employed in a more preliminary stage of the setup, namely during its design and construction. If a certain set of materials are to be studied, with a particular particle diameter and density, a unit can be built to match the desired operating conditions. The model will give a preliminary idea of what is possible to process in a certain unit, without experimental trials.

3.1. Fundamentals

This model was applied to three different materials – aluminium ($\rho_{Aluminium}$= 2700 kg.m^{-3}), alumina ($\rho_{Alumina}$= 4000 kg.m^{-3}) and high density polyethylene (HDPE; ρ_{HDPE}= 950 kg.m^{-3}) – and two different setup configurations – with swirl ratios of 30.94 and 27.27 – and it is based on a force balance made to a fluidized particle inside of a GSVR. This model strives to find the smallest particle diameter, of a certain material, that can be retained inside a certain GSVR, with a specific swirl ratio and dimensions. Henceforth, that variable will be called the critical particle diameter.

The critical particle diameter is the diameter that emerges from the balancing of centrifugal to drag force at a given radial position in a GSVR. Particles smaller in size than the critical diameter will be entrained from the specific radial position as the drag force will surpass centrifugal. As it was mentioned in the previous chapters, there are three main forces acting on a particle which is rotating in a GSVR: gravity, centrifugal – equation (3) – and drag force – equation (4). Gravity effects are assumed to be invalid for the present study (considering a vortex unit with a vertical central axis and placed horizontally). Hence, the force balance takes only into account drag (F_d) and centrifugal (F_c) forces, as presented below. As a rule of thumb, centrifugal force is believed to be the stabilizing one and drag to be destabilizing force for a vortex unit.

$$F_c = m_p \frac{v_{s,\theta}^2}{r} \tag{3}$$

$$F_d = \frac{1}{2}\rho_g A_p C_d u^2 \tag{4}$$

Where m_p is the mass of a single particle, $v_{s,\theta}$ is the azimuthal solid velocity, r is the radial position inside the chamber, ρ_g is the density of the gas, A_p is the cross-section area of the particle, C_d is the drag coefficient and u is the gas radial velocity.

Balancing both forces, three possible scenarios arise. In an ideal situation, drag and centrifugal forces will assume the same value, which results that the particle will keep a certain radial position inside of the chamber. However, during the operation of the GSVR, two more cases can happen. If the drag force exceeds the centrifugal force, the radial position of the particle will decrease and consequently, the particle will get entrained. If the centrifugal force exceeds the drag force, the particle will assume a

larger radial position. Hence, for a particle to stay inside of the reactor, the centrifugal force should be equal or higher than the drag force. That situation implies a minimum particle diameter, which is called the critical diameter since it is the smallest diameter a particle can assume in order to stay inside of the reactor. Equaling the drag and the centrifugal force and isolating the particle diameter in one member of the equation, equation (5) is obtained.

$$D_{cut} = \frac{3}{4} C_d \frac{\rho_g}{\rho_p} \left(\frac{v_{g,r}}{v_{s,\theta}}\right)^2 r \quad (5)$$

Equation (5) is the core of the presented model. Knowing every variable in its right side, one can calculate the critical diameter for a set of material-reactor pair. This equation gathers characteristics of both. ρ_p and $v_{s,\theta}$ are linked with the material itself, while ρ_g, r and $v_{g,r}$ are related with the setup configuration. C_d is a variable which gathers the influence of both. A description on how to determine each parameter will follow.

C_d is the drag coefficient which depends on the flow regime, and therefore on the Reynolds number. In this context, the Reynolds number is modified for the particle Reynolds number – equation (7). There are several correlations for determining C_d, which criterion of use is usually a range of the Reynolds number, and the chosen one is presented in equation (6)[63]. Similar approach was used by the works of De Weber et al[45] in their study of segregation in a GSVR.

$$C_d = \frac{24}{Re_p} + \frac{2.6\left(\frac{Re_p}{5}\right)}{1+\left(\frac{Re_p}{5}\right)^{1.52}} + \frac{0.411\left(\frac{Re_p}{263000}\right)^{-7.94}}{1+\left(\frac{Re_p}{263000}\right)^{-8}} + \frac{0.25\left(\frac{Re_p}{10^6}\right)}{1+\left(\frac{Re_p}{10^6}\right)}, 0.1 < Re_p < 10^6 \quad (6)$$

$$Re_p = \frac{\rho_g d_p v_{g,r}}{\mu_g} \quad (7)$$

There were other correlations that could have been used in this case, but this was the one with more information available on the literature and the only one applied in the same context, by Weber et al[45] . Some other correlations were applied but the outcoming results converged for a trivial solution – particle diameters tending to zero and were hence ignored.

The velocities present in equation (5) – $v_{g,r}$ is calculated from equation (8) – while the $v_{s,\theta}$ values are taken from PIV trials reported by Gonzalez-Quiroga et al.[64] done with Aluminium particles with 500 μm. Because the reported azimuthal solid velocities are local ones, and not averaged, it was decided that the values should be approximated using a linear regression. Thus, the outcoming results will be an average of all the particle diameters found at a certain radial position in the chamber.

$$v_{g,r} = \frac{G}{2\pi r L} \quad (8)$$

The setup used by the work of Gonzalez-Quiroga et al.[64] is different from the one depicted in chapter 2. Table 1 is presented with all the relevant information about that setup.

Table 1. Dimensions of the setup used for the PIV trials reported by Gonzalez-Quiroga et al.[65]

Variable	Value
Radius chamber	80 mm
Height chamber	15 mm
l_N	8
l_0	1 mm
α	10º
Swirl Ratio	30.94
Exhaust Diameter	40 mm

Since C_d also depends on the particle diameter, the presented equation cannot be simply solved. Therefore, an iterative process was employed to determine the critical diameter for each case. First, a particle diameter was chosen for each evaluated material. For aluminium, the initial value is the same as the used by Gonzalez-Quiroga et al.[64]. For alumina, the value chosen was 600 µm, a typical particle size. Then the particle Reynolds – equation (7) – and the drag coefficient – equation (6) – were calculated with that value. Finally, a new particle diameter was calculated using equation (5). The procedure was repeated for several gas flow rates, radial positions and materials. The results are shown in the next figures – Figure 9 and Figure 10. Since it is an iterative process, it must have a stop criterion. For both materials, it was decided that the iterations could be stopped when, for two consecutive calculations, the outcoming particle diameters differ in 5 µm or less.

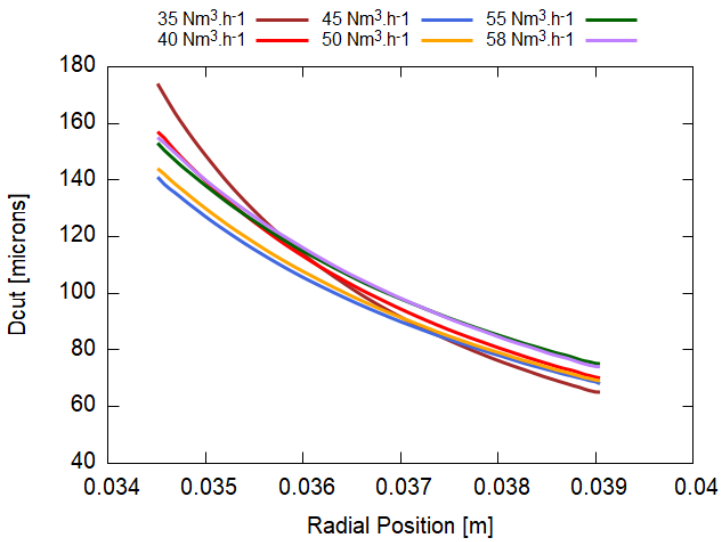

Figure 9. Critical aluminium diameter along the chamber for several gas flow rates.

The data in Figure 9 can be interpreted as follows: the minimum aluminium particle diameter that can be retained inside a reactor with the same characteristics and using 35 $Nm^3.h^{-1}$ of air is approximately 70 µm. And if the largest bed formed by aluminium particles that can be retained is 4.5 mm, then the smallest particle diameter that is possible to retain in the bed, under the same air flow rate, is approximately 170 µm.

To apply the same method to other materials, an assumption has to be made. For alumina, a momentum balance is necessary, since there is no data available regarding the azimuthal velocities of such materials in a GSVR. The momentum transfer from the gas phase to the solid phase in a GSVR depends on the swirl ratio, the main gas flow rate and the gas properties. Thus, maintaining such conditions, e.g. using the same reactor, the same gas phase, and the same gas flow rate, the momentum balance associated to the solid phase can be described by equation (9).

$$(v_{s,\theta} m_p)_{\text{Aluminium}} = (v_{s,\theta} m_p)_{\text{material}} \quad (8)$$

Since the properties (density and size) of the particle are known, it is possible to calculate the azimuthal solids' velocity of that material and therefore determine the critical particle diameter for each radial position and gas flow rate – Figure 10.

The momentum balance described in equation (8) is not valid for all materials. When the compared materials differ in terms of fluidization classification under centrifugal forces, then equation (8) cannot be applied. What is known is that the momentum transferred by the gas is always the same, since the air properties and the gas flow rate used remain unaltered. But each material receives that momentum in a different way, which is thought to be correlated to its fluidization patterns and behavior. That momentum can be converted into azimuthal velocity (remark that in a GSVR, it is assumed that the solid phase does not have radial velocity) or it can be lost through friction – mainly between the particle and the circumferential walls).

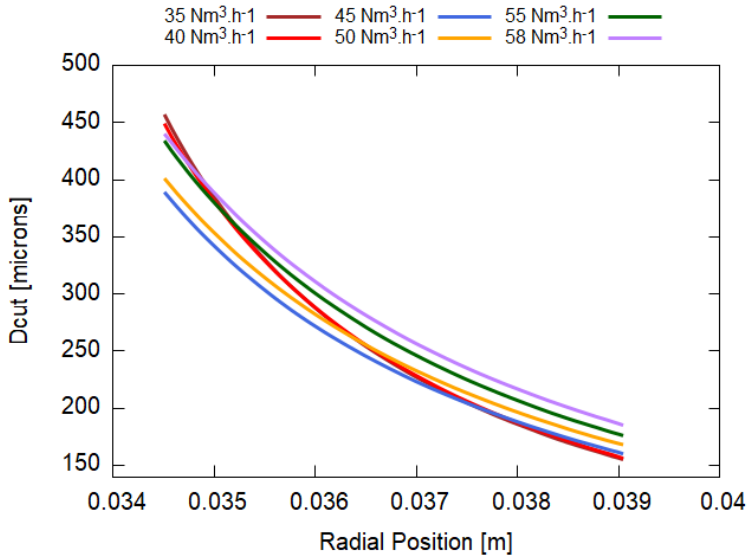

Figure 10. Critical alumina diameter along the chamber for several gas flow rates.

Figure 10 can be analyzed in the same way as Figure 9. If the unit is empty and a flow of 35 $Nm^3.h^{-1}$ of air is fed to the chamber, an alumina particle with 160 μm is the estimated minimum particle size that can be retained in the reactor. As the operator feds more particles, a fluidized bed starts to form and to expand. If the maximum bed length that is possible to achieve in this reactor and using the

same air flow rate has approximately 5 mm, the biggest alumina particle that can be kept inside is estimated to have around 450 μm.

Comparing both materials, alumina presents values for the critical diameter larger than aluminium. That difference has mainly to do with the difference of densities between the two materials. The denser the material, the heavier the particles (while keeping the size unaltered) and harder is to keep them inside of the chamber. A heavier particle will have a higher mass, and, for that reason, it would be expected for that particle to sense a stronger centrifugal force. But the azimuthal solid velocity will decrease for denser particles[23]. And since that variable is squared, it influences more the outcoming value for the centrifugal force then the mass of the particle, which is only directly proportional. Therefore, the centrifugal force will not increase, but decrease, causing the particles to assume a smaller radial position, being closer to the exhaust and therefore, more likely to be entrained from the chamber. To balance that drop on the azimuthal solid velocity, the particle must assume a higher size, which results in higher mass but also higher projected area, increasing the drag force. The whole set of reasons explained in this paragraph justifies why a denser particle has to be bigger in size to be able to stay inside a GSVR. Besides density, there are other variables that have an impact on the resulting critical particle diameter. Therefore, a sensitivity analysis is performed and presented in Figure 11.

3.2. Evaluation of the Model

The developed model was depicted in the last pages and its results applied to two different materials shown. After that, the model should be evaluated, in terms of its robustness. For that purpose, a sensitivity analysis was performed to the main variables which affect the critical diameter – the azimuthal solid velocity, the radial gas velocity, the particle Reynolds and the drag coefficient. The sensitivity analysis was performed only to one material. Although the method was based on experimental PIV data, the opportunity to apply the model to a new set of conditions arose. This is a way to assess the range of conditions where the model can be applied.

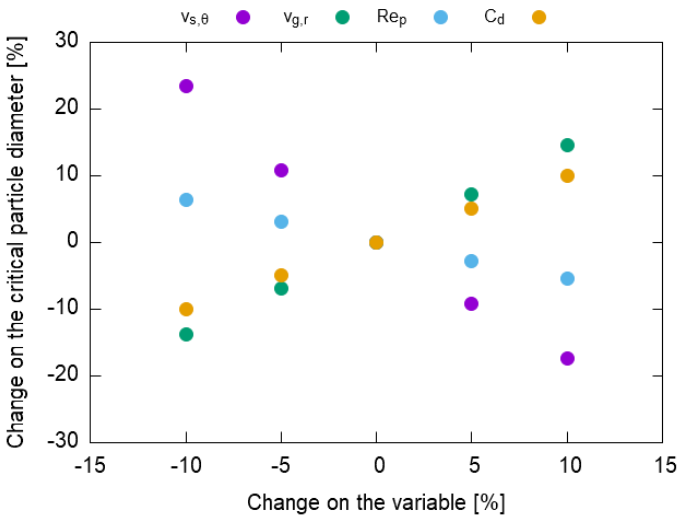

Figure 11. Sensitivity analysis on the particle diameter.

A sensitivity analysis was performed for aluminium – Figure 11 – , choosing one radial position – 0,0345 m – and one gas flow rate – 35 $Nm^3.h^{-1}$ – in order to evaluate which parameter influences greatly the critical diameter. For that purpose, positive and negative changes were done in the variables present in equation (5) and the outcoming results compared with the initial scenario. Using such process, it is possible to conclude that the particle Reynolds does not influence significantly the particle diameter (the changes induced by modifying the variable on the evaluated range are always smaller than 10%), while the azimuthal solid velocity has a greater influence on the particle diameter, in the studied range – a change of -10% on this variable causes the particle diameter to increase in more than 20%.

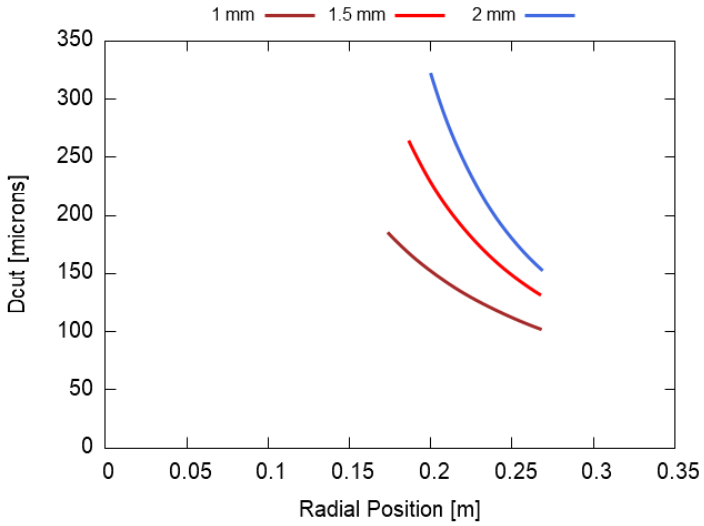

Figure 12. Resulting trends for the D_{cut} along the bed by using the model with different approximations for the initial value of particle diameter.

Besides evaluating the effect of several variables on the outcoming particle diameter by doing a sensitivity analysis, as described in the last paragraph, the influence of the initial approximation which initiates the iterative method was also studied. For that purpose, the developed mathematical method was applied to three different initial set of conditions. HDPE particles with several sizes are fed to a GSVR, and the azimuthal velocities of the particles are calculated using PIV data – Figure 13. According to the preformed sensitivity analysis, this parameter plays an important role in the accuracy of the critical particle diameter. Using the data obtained by Kovacevic et al., a second point of view on the sensibility of the model is given.

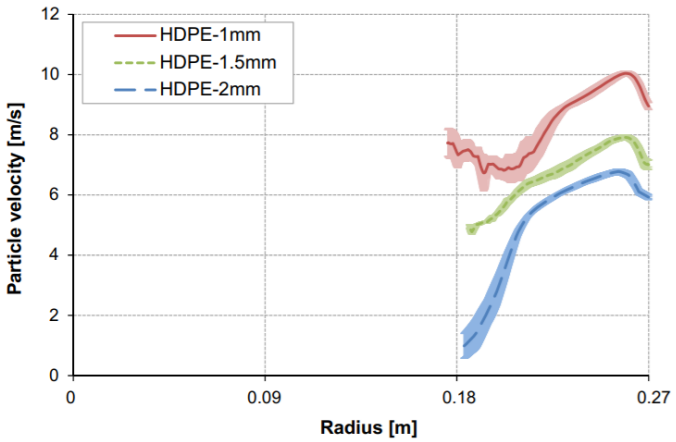

Figure 13. Azimuthal velocities along the bed for several particle sizes[23].

Using the data presented in Figure 13, which was processed by an online tool – WebPlotDigitizer – the model was applied to the three different set of conditions. Each described set will be the starting point of the iterative method. For a matter of congruence, the azimuthal solid velocities collected from Figure 13 were linearized and the outcoming values used to calculate the critical diameters. Taking into account that only the density of the material has a direct influence on the outcoming result, as it is directly proportional to the drag force, applying the iterative method to the three presented cases should result in similar final values for the critical diameter, for all the radial positions evaluated

If the reader gives a closer look to Figure 12, will see that is not the case. The resulting curves for each initial approximation are considerably different, predicting critical diameters which differ in more than 150 μm for r=0.21 m. The larger the initial approximation for the critical diameter, the larger the predicted D_{cut}. The difference between the curves gets smaller as the radial position increases, e.g. the particle gets further from the exhaust. For the largest radial position, the results given by the method differ in approximately 50 μm. All the curves appear to converge to the same value, which will be the minimum diameter that an HDPE particle can have to be fluidized in an empty GSVR.

Another aspect worth to be mentioned is that the measured azimuthal velocities presented by Kovacevic et al. are not for the same range of radial positions. The smaller the particles, the larger gets that range, which is nothing less than the height of the fluidized bed and a portion of the freeboard region.

3.3. Limitations

While evaluating the robustness of the mathematical model, the reader can already perceive that its range of applications is limited, mainly for mathematical reasons, as it is expressed by the sensitivity analysis and the application of the method to an experimental set of values.

The main reason for the results given by the sensitivity analysis is that the model is developed based in only one set of conditions, obtained in one setup with a constant swirl ratio, for a specific

material and a certain range of gas flow rates. For it to have a broader range of applications, it was necessary to base the method in more experimental values, retrieved from several setups and fluidizing different materials with different sizes. During the next paragraphs, several limitations associated with the model will be depicted.

The model was developed using only Excel, which has a limited capacity when it comes to iterative processes. There were some mathematical problems with convergence, since the model tended to converge to a trivial solution. During each iteration, a new air of values for the particle Reynolds and the particle diameter where calculated. As the iterations continued, the particle diameter would converge to zero and the particle Reynolds would increase to extreme high values, e.g. converge to infinite.

An attempt to overcome the convergence problem was to find more correlations for the drag coefficient. A total of 5 correlations – Table 2 where tested but only one gave results which converged for satisfactory values. That correlation was already reportedly used for a similar work (Weber et al.) although its performance for predicting drag coefficients in GSVR's is not yet tested. One of the five correlations used was created especially for GSVR's[66] , but it was concluded that this correlation was not suitable for this mathematical model. This correlation depended on different variables. A new definition for the Reynolds number is used, which is called radial particle Reynolds number, $\mathrm{Re}_{p,R}$. This is a more accurate way to define the Reynolds number in a GSVR. Besides this variable, the bed porosity and the swirl ratio integrated the expression too. When this correlation was applied to the system in study, the resulting particle Reynolds numbers were too small when compared with the ones present by Friedle et al[66]. In Table 2, all the correlations that were tested are presented. For that reason, that correlation was discarded.

Table 2. Set of correlations tested. The marked correlation was the one used.

Reference	Expression
Stokes' Law	$\frac{24}{\mathrm{Re}}$
Ergun	$150\frac{(1-\varepsilon)^2}{\varepsilon^2}\frac{\mu_f}{d_p^2}+1.75\ \frac{(1-\varepsilon)}{\varepsilon}\frac{\rho_f}{d_p}(u_i-v)$
Rowe and Henwood[67]	$\frac{24}{\mathrm{Re}}\ (1+0.15\mathrm{Re}_p^{0.687})$
Friedle et al.[66]	$(15\pm4.65)\varepsilon^2\mathrm{Re}_{p,R}^{-0.28\pm0.05}S^{0.76\pm0.03}$
Morrison, F. A.[63]	$\frac{24}{\mathrm{Re}_p}+\frac{2.6\left(\frac{\mathrm{Re}_p}{5}\right)}{1+\left(\frac{\mathrm{Re}_p}{5}\right)^{1.52}}+\frac{0.411\left(\frac{\mathrm{Re}_p}{263000}\right)^{-7.94}}{1+\left(\frac{\mathrm{Re}_p}{263000}\right)^{-8}}+\frac{0.25\left(\frac{\mathrm{Re}_p}{10^6}\right)}{1+\left(\frac{\mathrm{Re}_p}{10^6}\right)}$

Another aspect to account is that since the model is based on aluminium azimuthal velocities it can only be extrapolated for materials which centrifugal fluidization classification is the same as aluminium. Otherwise, the momentum balance stated in equation (8) can no longer be valid, since the fluidization mechanisms are also different. Thus, the model can only be applied to other materials if 1)

they have the same centrifugal fluidization classification or 2) when there is available data, namely radial positions vs. azimuthal solid velocities for a certain particle size of such material.

There are some approximations done between iterations. The azimuthal solid velocities should change between each iteration, since a new step on the iterative process leads to a new particle size. Something else that also changes with the particle size is the bed height that should be evaluated. As the particle decreases in size, the bed height expands radially inwards (the centrifugal force will decrease for a smaller particle because its mass will also decrease). This approximation is supported by Weber et al., who presented the same reasoning but contradicted by Kovacevic et al., whose results show a significant difference between the azimuthal solid velocities of particles with different velocities from the same material. As we change the size of the particles, the solid volume fraction also changes, as shown in Figure 29. This change will produce a variation of the bed height, which is also not accounted in the model.

The model was designed to a specific reactor, with a certain swirl ratio (the geometry of the reactor was kept constant during all the trials), since all the experimental data was retrieved from the same setup, the one described in Table 1. Applying the model to other GSVR can lead to erroneous results. The same problem exists when it comes to the valid range of gas flow rates.

Lastly, the preformed force balance was done to a single particle. Interactions between particles or particle-wall were not accounted, nor its effects. Although the entire bed height has been accounted, the existence of more particles (which are the reason why the bed grows inwards radially) are not taken into account. This approximation can influence the drag coefficient, which is probably underestimated.

3.4. Conclusions

The modeling work developed under the scope of this master thesis resulted in a successful mathematical model which can preliminarily estimate the minimum particle diameter of a certain material that can be fluidized in an empty GSVR. The method has several limitations, but it can safely be extended to materials which have the same fluidization behavior as aluminium, under centrifugal forces.

This model can be used for designing purposes and for studying theoretically which materials of which size can be processed in an already existing unit. For achieving accurate results, a great quantity of data, namely azimuthal solid velocities, should be given to the model. This variable is the one that most influence the accuracy of the critical particle diameters. This model gets the scientific community one step further to comprehend the hydrodynamics of the GSVR.

4. Vortex Setup Description and Experimental Methods

The vortex setup consists of 3 sections: the gas-solid feed section, the Gas Solid Vortex Unit (GSVU) section and the downstream section, as identified in Figure 14.

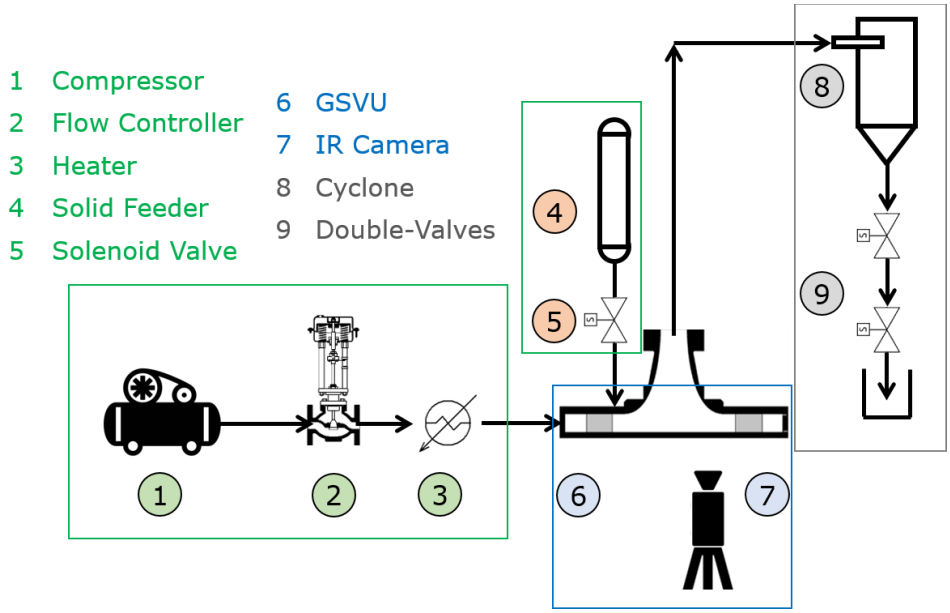

Figure 14. Schematic view of the vortex setup, highlighting three sections and key elements within each of them.

4.1. Gas-Solid Feed Section

Gas (compressed air for the present study) is supplied to the unit via a compressor (Atlas Copco, GA90VSD, with a maximum working pressure of 13 bar (g)), at a pressure of 4 – 5 bar (g). A thermal mass flow controller (Bronkhorst F-106 CI series) delivers 20 – 600 $Nm^3\ h^{-1}$ gas to the unit; for pressures between 1 – 2 bar (g). Metered gas can be directly sent to the unit at room temperature (i.e. “Cold” experiments) or can be heated by an electric heater. Nine internally finned tubes, with individual temperature control, serve as the gas heater assembly. Hot/cold gas gets distributed in 8 corrugated plastic hoses (glass fabric impregnated with silicone and exposed steel coil, maximum temperature of 260 °C). These tubes are connected to the sides of the unit to form an octagonal jacket. An image of the gas-feed section is presented in Figure 15 (a).

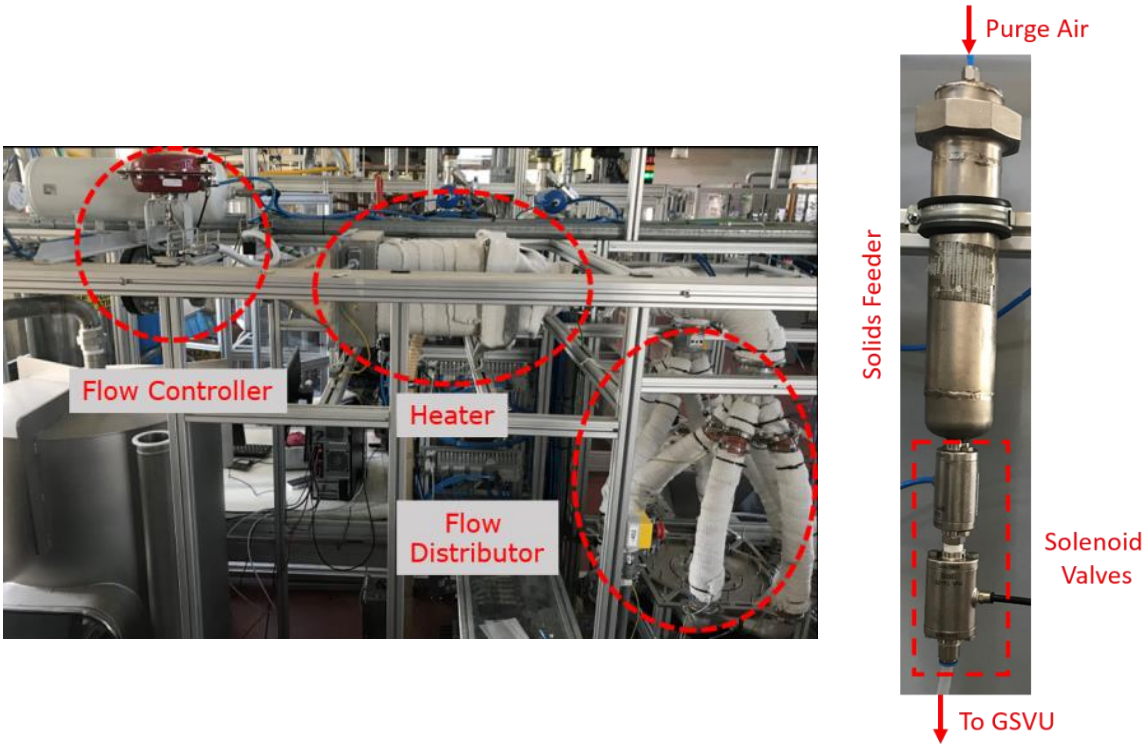

(a) (b)

Figure 15. (a) Gas-feed and (b) Solid-feed sections of the GSVU.

Solid, on the other hand, are fed to the unit via a pneumatic conveying assembly, assisted by a minimal flow of compressed air. Solid for feeding are stored in a closed stainless steel vessel (maximum capacity of 2 kg), with a connection for purge air flow. From the vessel, a transparent polyurethane tube (internal diameter of 6 mm) is connected to one of the end-plates (discussed later) of the unit for feeding particles to the unit. A solenoid valve on the feeding tube inhibits gas backflow from the unit to enter the solid feed vessel. The purge air flow can be varied depending on the particle properties used in the experiment. However, the purge flow is typically set to a low value (< 3%) so that the additional air flow does not influence the behavior of main gas flow (coming from the jacket). Figure 15 (b) shows solid feed section in brief.

4.2. GSVU Section

Gas entering the octagonal jacket gets distributed to 16 concentric vanes (Stainless Steel or Polyamide), arranged in a circular fashion as shown in Figure 16. The openings between two successive vanes act as slots of varying slot sizes (0.5 – 1 mm). Slot openings are angled at 2.5° w.r.t. the tangent to the chamber. The inner edges of vanes form the unit chamber with a diameter of 139 mm. The outflowing gas and solid exit the unit via the common central outlet. A transparent silicone pipe connects the unit to the cyclone separator downstream. Figure 16 (b) (1) presents the top view of (vertically downwards exhaust) unit chamber and vanes arrangement.

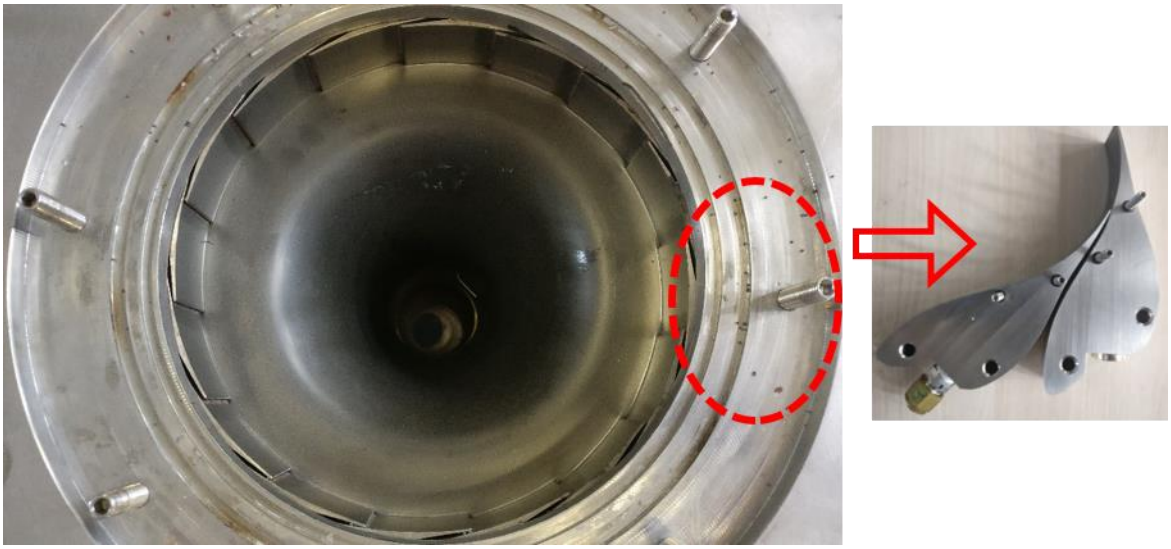

(a)

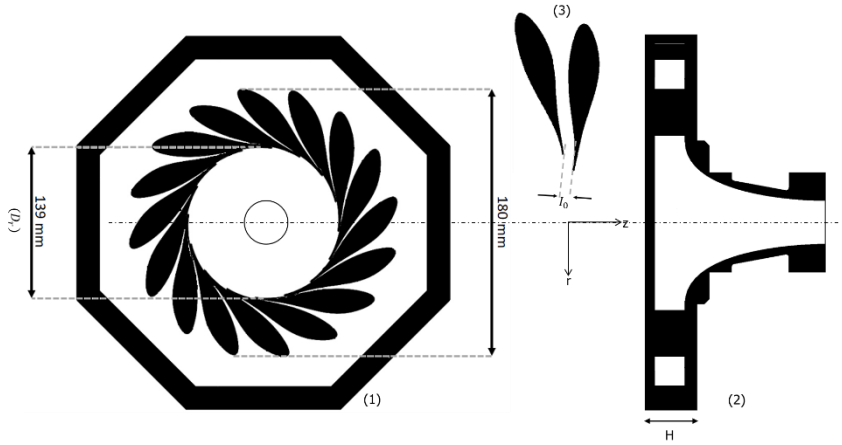

(b)

Figure 16. (a) Top view of the unit chamber (inset: top view of two adjacent metallic vanes forming a slot) and (b) schematic of the unit: (1) Top view; (2) Side View and (3) adjacent vanes forming a slot.

Two Stainless Steel end-plates are placed at an axial distance of 25 mm, forming the length of the unit. One of the end-plates centrally holds the exhaust for both gas and solid particles. The other plate has a multifunctional design consisting of 4 quadrants. One of the quadrants holds the pressure sensors assembly used to measure solid bed pressure at various radial positions, as shown in One absolute pressure sensor, located at the outermost radial position (r=69 mm), is used as the reference. Based on this reference value, differential pressures at nine (9) other locations towards the exhaust can be measured and recorded. These differential sensors are positioned at radial positions 3 mm apart (between r=66 mm to r=42 mm). A second quadrant holds the solid inlet tube. The inlet connection is positioned at a 45° angle w.r.t. the end plate for an easy feeding to the unit. The tube is angled along the solid flow direction inside the unit. The inlet line holds a converging Teflon insert with a 3-4 mm opening in the chamber. The insert assists solid feeding to the unit, at the same time acting as a non-return valve and avoiding the backflow of main gas into the solid feeding line. The solid feeding port is

located at a radius of 62 mm. The remaining two quadrants can be used for providing visual access to the unit internals. Makrolon® (for room temperature experiments) and Pyrex or Zinc Selenide (for high temperature experiments) plates are used for the visualization purpose. These transparent plates can be used to measure radial bed height or the solid velocities using Particle Image Velocimetry (PIV). Owing to the mechanical abrasion due to high shear and recurrent contact with particles, these plates need to be regenerated or replaced frequently. All the quadrants have a modular design and can be interchanged independent of each other as the application demands. The unit also has flexibility in orientation and can be operated in two modes: (1) exhaust aligned with gravity and (2) exhaust against gravity. Both these modes have their advantages and shortcomings, which will be discussed later in this chapter.

4.3. Downstream Section

Solid entrained with the exiting gas are introduced to a cyclone separator installed downstream the unit, as presented in Figure 18. Separated solid are recovered at the bottom of the cyclone, while gas is vented off. An air-actuated double-valve assembly at the bottom of the cyclone separator allows solid recovery during operation, without any pressure or flow disturbances in the unit.

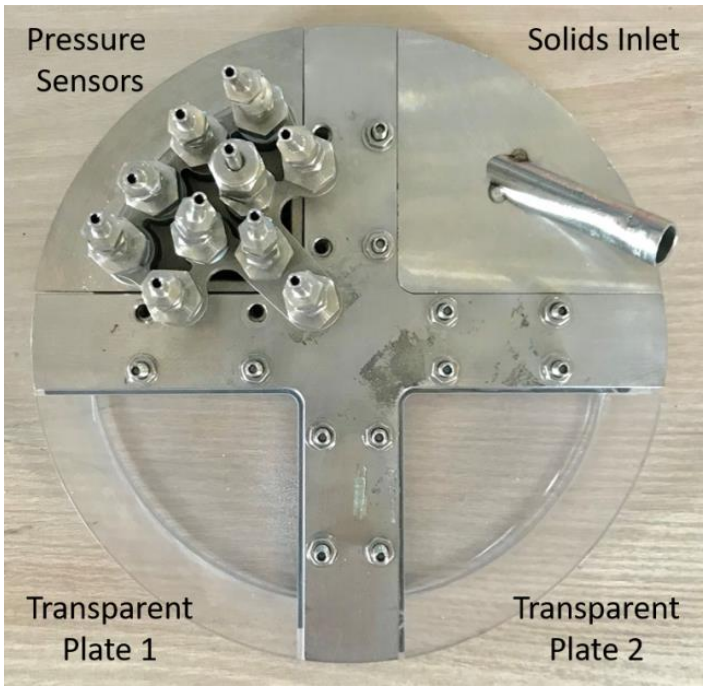

Figure 17. Unit end-wall assembly.

Valves opening-closing, flow, temperature, etc. can be set and operated using the Siemens operating software (control system). All sensor values are logged at a frequency of 10 Hz and stored in *.csv* files and can be used for further post processing.

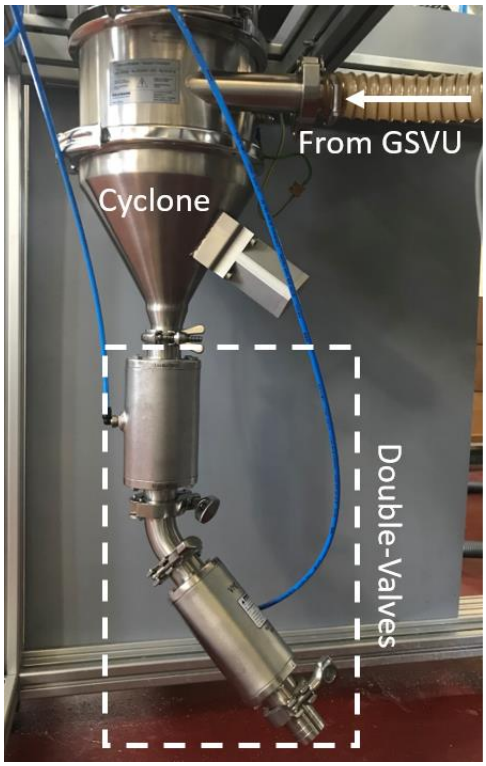

Figure 18. Downstream section of the unit.

To successfully perform all the planned experiments, some changes were made in the setup. Improvements in the solids' feeding and collection were a compulsory requirement, in order to reduce the material losses. In the feeding system, an On-Off valve was installed to control the flow of the solid phase. Regarding the collecting system, it was assembled from scratch. This upgrading enables the operator to separate both phases. Both phases would go through a cartridge filter, which had attached a shaker, where the gas phase would flow through a vent and the solid phase would pass by a two-valve system and finally be collected.

4.4. Experimental Method - Maximum Loading

The adopted procedure for studying the maximum loading of aluminium particles in a vortex reactor is explained below. Three main air flow rates are used: 80, 100 and 120 $Nm^3.h^{-1}$.

1. Feed, through the inlet of the top plate, a pre-weighed quantity of solids to the reactor. If the operator thinks the fed quantity is smaller than the maximum loading, feed a known quantity of the same material afterwards.

2. Wait for approximately 5 minutes or until the bed is stabilized. If the bed still presents some irregularities in flow patterns, like slugging, more solids should be added. Once again, the total amount of solids should be known. Wait until the bed is stabilized.

3. Collect the solids present in the collecting box, placed underneath the exhaust. That quantity is named as the ‘entrained quantity’. Weight that quantity for mass balance closure. This step should only be performed if a significant amount of solids is present in the collecting box. Otherwise, repeat step 1.

4. Clean the solids inside of the reactor. Turn the gas flow rate to a lower value to take all the solids out of the reactor. If any solids remain, drag those particles through the exhaust using compressed air.

5. Collect the solids in the collecting box. That quantity is named as the ‘maximum loading’ for a certain material and for a certain air flow rate.

6. Repeat the procedure three times or until concordant values are achieved to assure accuracy and to obtain averaged values and corresponding standard deviations.

4.5. Experimental Method - Particle Segregation/Mixing

To study this phenomenon, aluminium and alumina particles of different sizes (0.7-1mm diameter), were used. Mixtures of two different sizes and several compositions (0, 25, 50, 75 and 100% of a certain size) were fed to the reactor. The total mass of the mixtures is always kept at 100 grams. Three main air flow rates are used: 80, 100 and 120 $Nm^3.h^{-1}$ and the purge air was kept at 500 mbar. Next, the adopted procedure is depicted.

1. Feed a known mixture (e.g. the composition and the used particle sizes) to the feeder.

2. Turn on the purge air to pressurize the solids feed vessel.

3. Open the valve downstream the feeder. The solids will leave the feeder, pass the connecting tube and enter the reactor. From this moment, wait for 5 minutes, so a stable bed is achieved. Tap the inlet of the top plate to help the solids to enter (in case the feeding tube gets blocked). Shake the feeder to assure that all the solids are fed to the reactor. During the waiting time of 5 minutes, three measurements of the bed height were taken. The pressure sensors along the bed should be on from this moment and until the end of the trial.

4. When the bed is visibly stabilized, turn the shaker on, close the top valve and open the bottom one, collecting the solids that were entrained in a cup. Once the collection is finished, turn the shaker off, open the top valve and close the bottom one. This arrangement ensures collection of entrained solids without the need of stopping the main gas flow via the reactor.

5. Sieve the entrained quantity to separate particles from different sizes. Weight each fraction.

6. Reduce the gas flow rate to a minimum, causing the remaining solids to leave the reactor. Some solids can stay inside. To remove those, insert the compressed air gun at the inlet of the top plate and press it until there are no particles in the chamber.
7. To collect possible solids in the tube between the reactor and the cyclone, turn the air flow rate to its initial value.
8. Once again, turn the shaker on, close the top valve and open the bottom one. Collect the ‘retained solids’ in a cup.
9. Sieve the retained quantity to separate particles from different sizes. Weight each fraction.

5. Experimental Results and Discussion

5.1. Maximum Loading

Experiments have been done to understand the influence of the position of the exhaust in the hydrodynamics of the setup. Results were compared with the work reported in another thesis[11]. During the work, the unit was assembled in such a way that the exhaust was positioned against gravity. In the present case, the setup was rotated such that the exhaust was aligned with gravity (facing vertically downwards). The maximum loading was evaluated for the new exhaust configuration at three different flow rates of the common fluidizing agent, i.e. compressed air: 80, 100 and 120 $Nm^3.h^{-1}$. The purge air required to push the solids into a developed a gas flow in the unit was kept at a constant value of 600 mbar pressure and contributes to a negligible fraction of the main gas flow All the trials were performed at room temperature and using non-porous spherical particles of Alumina ($\rho_{Alumina}$=4000 $kg.m^{-3}$, d_p=0.7-0.8 mm) as solid phase.

The results of such experiments are presented in Figure 19 and compared with the results of the experiments done with the exhaust assembled against gravity.

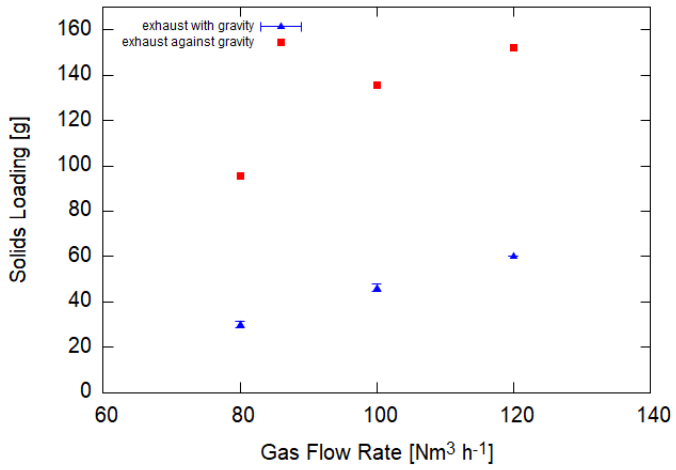

Figure 19. Maximum loading of Alumina (0.7 – 0.8 mm) for several air flow rates. Blue: Average data points and error bars for the exhaust orientated with gravity. Red: Average data points for the exhaust orientated against gravity.

The maximum loading can be defined, for a given flow rate, as the mass of solids in the bed/reactor beyond which there will be particles leaving through the exhaust. During experiments, some patterns were noted. For all the experiment conditions, there were always solids in the freeboard region, arranged in the shape of a vortex. The solids that reach that region will certainly leave the reactor at some point. The effect of gravity also obeys to a pattern: for lower airflow rates, both the centrifugal and the drag force are smaller, but gravity does not change. Consequently, it is observed a thicker bed in lower axial positions, since the particles are being pushed down. For higher air flow rates, this effect is much less visible. We concluded that at any air flow rate, the bed would stabilize in, approximately, 5

minutes. For higher flow rates, the bed also presents itself as thinner and uniform. Since the solids are fed through a unique inlet at the top plate, the portion of the bed that is on the same direction is always thicker than the rest of it. This effect is more visible for lower gas flow rates, being almost irrelevant when higher gas flow rates are used.

Observing the results from both experiments, it is clear that the higher maximum loading is achieved for the previously studied configuration. In the current arrangement, the particles are pulled through the exhaust because of gravity. It is observed that even minor changes to solids rotating closer to the exhaust, brought about by either collisions or miniscule changes to the gas flow rate, the particle tend to leave via exhaust, under added influence of gravity. This effect does not happen in the previous configuration once the exhaust is against gravity. When the exhaust is oriented vertically downward, gravity effects start to dominate in the freeboard zone as well as in the backflow zone. As a consequence, the presence of freely rotating particles in the freeboard are no longer observed in this mode of operation. The lack of loosely rotating particles in the unit suggests that all solid are accommodated in the bed, unlike in the previous mode. Furthermore, deposition of particles on the bottom plate is not possible due to strong gravitational effects on heavy particles such as Alumina. As a combined effect of both, the maximum solid loadings are substantially lowered when operating with an exhaust aligned with gravity. With all other operating conditions being unchanged, roughly half the amounts of solid can be retained in the configuration with downwards exhaust. Smaller error bars on the solid loadings across all the flow rates is also resultant from the lack of solid lingering on the bottom plate, as opposed to the previous configuration.

The experiments presented in Figure 19 demonstrate the flexibility of the setup in terms of various operating modes, ease of feeding and recovering solids (in accurate fashion, for quantification purposes) and stable operation over long time periods. It also shows that for achieving a larger solid loading, the studied unit should be orientated with the exhaust against gravity.

5.2. Particle Segregation/Mixing

As explained in the first chapter of this thesis, particle segregation is a characteristic of vortex reactors. Particles with different mass, due to diameter or density, will have different radial positions inside of the chamber, since they have different values of centrifugal and drag forces. Hence, in a GSVR, the probability of particle entrainment will be higher for particles which radial position is smaller, e.g. closer to the exhaust. Therefore, lighter particles are more likely to leave the reactor, in opposite to heavier particles. To study this phenomenon, the composition of the bed was examined by analyzing the entrained and retained quantities and their composition. During operation, some characteristics of the bed were also studied, such as the bed height and the pressure drop across the entire reactor. Those measurements were an attempt to gather more information related with the system.

A lot of information can be retrieved from such experiments. With data coming only from the weights of both fractions, only qualitative appreciations can be made. In the following pages, plots which

were considered to be relevant are present and depicted. Some qualitative relations are extracted from those figures.

Two types of mixtures with different materials were prepared. The first contained only alumina particles in two different sizes, 0.7-0.8 mm and 1 mm. By doing experiments with such mixture, the influence of size in the particle mass, the driving force for particle segregation in a GSVR, was to be evaluated. The second mixture was composed by two different materials, alumina and aluminium, with 1 mm and 0.7 mm particles, respectively. This time, the combined effects of changing density and size in the solid phase were evaluated. The effect of density was coupled with the effect of size because of practical reasons. The particles available at the time of the experiments were not easily separable by magnetism (neither alumina or aluminium have magnetic properties) or density (for example, using a liquid or a solution which density was in between the density of both materials). Therefore, the effects of both properties were not studied apart. Although, this second set of experiments was designed in order to change only the density of the small particles, since the size and density of the larger particles is the same as the one used before. For that reason, it is acceptable to suppose that the changes observed in these experiments are mainly due to effects of density.

Both mixtures were processed using a common procedure, already described in the beginning of the chapter. Firstly, graphs which can be compared are presented, side by side, to ease the comparison. For all the experiments, F1 refers to larger fraction (i.e. 1 mm Alumina particles). F1/F2 refers to the mass ratio of larger to the smaller particles (in bed).

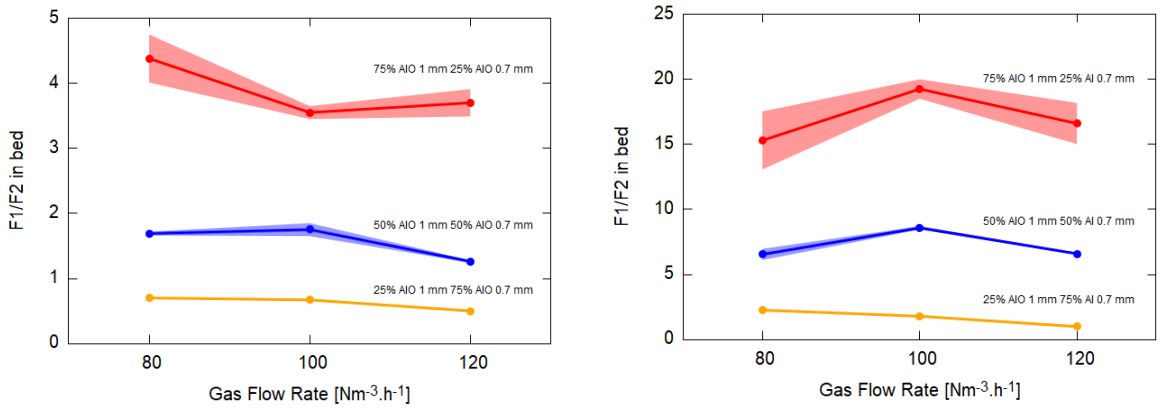

Figure 20. Ratio between (a) 1 mm and 0.7-0.8 mm alumina particles retained in the bed for several gas flow rates; (b) 1 mm alumina particles and 0.7 mm aluminium particles retained in the bed for several gas flow rates. The indicated percentages are reported with respect to 1 mm alumina particles in the initial mixture. (colored areas represent respective error region)

According to Figure 20 (a), for the same gas flow rate, the ratio F1/F2 in the bed suffers great changes when the initial mixture composition is changed. But for the same initial composition, that parameter does not present significant changes when subjected to different gas flow rates. Therefore, the initial composition of the fed mixture plays an important role in the matter of the composition of the fraction retained in the reactor. When the amount of larger particles fed increases, the studied ratio

increases as well. Beyond a smaller impact, the influence of the gas flow rate does not follow a clear trend on the studied range. For the case where the mixture is composed of 75% of 1 mm particles, the outcoming values for the mass ratio are much bigger than for the other two compositions. That means that in that case it is possible to incorporate a large quantity of 1 mm particles, diminishing the amount of smaller particles, which has a double effect on F1/F2, increasing it even more than expected.

Figure 20 (b) corresponds to Figure 20 (a) to the other set of experiments (aluminium-alumina mixture). In general, the ratios obtained for a mixture of particles with different densities and sizes are approximately 5 times larger than the situation where only sizes are different (except for the 25% initial composition). Such difference is both due to an increase of alumina particles retained in the bed and a decrease of smaller particles. Larger particles are more easily retained in the bed. Therefore, these particles will occupy more space, leaving less space to be filled by smaller particles. This behavior causes an immense increase in the evaluated ratio.

As before, the ratio between particles of different nature increases with the amount of bigger particles in the initial mixture. This trend is a result of the initial mixture itself. The larger the amount of bigger and heavier particles available, the larger will be its mass fraction in the bed. As stated before, heavier particles are easier to retain in the GSVR than lighter particles, which leads to beds mainly composed by larger and denser materials.

Concerning the influence of the air flow rate in the ratio of particles retained in the bed, the conclusion is the same – the gas flow rate does not significantly change the composition of the bed and its effect does not follow a clear trend. This parameter is known to influence greatly the total mass of the bed, but not its constitution. Albeit, there is one clear difference between the two graphs. The trend followed by the mixture with the highest composition in alumina shows some disparities, linked with the point corresponding to the smallest flow rate and the highest composition in alumina. This mixture is also the one that shows larger error bars, which indicates that the fluidization of such mixture is perhaps less stable than the others, producing less precise results.

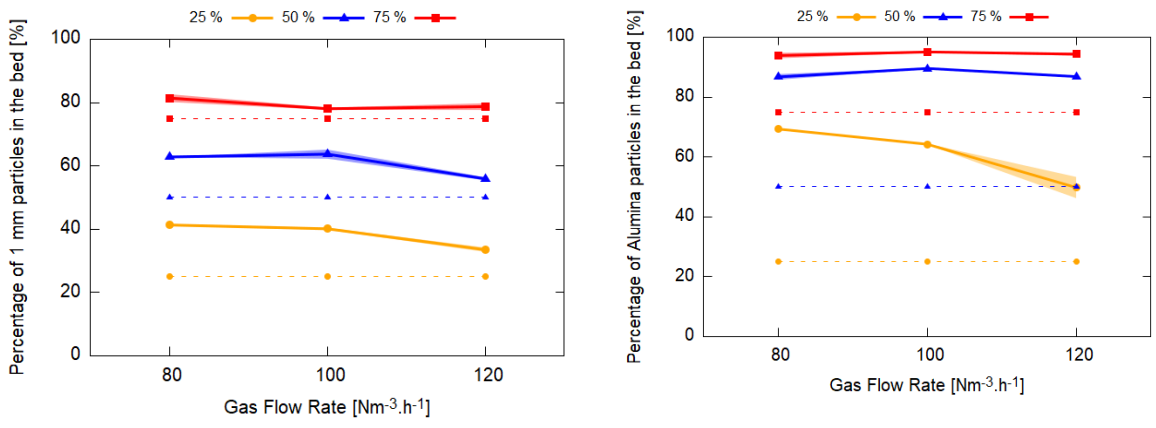

(a) (b)

Figure 21. Fraction of 1 mm particles retained for various mixtures with different mass compositions. (a) Fed mixture composed by 1 mm and 0.7-0.8 mm Alumina particles; (b) Fed mixture composed by 1 mm Alumina particles and 0.7 mm Aluminium particles. Colored areas represent respective error region. The dashed lines represent the initial compositions with respect to 1 mm particles.

Observing Figure 21 (a), the main gas flow rate does not appear to greatly influence the fraction of 1 mm particles retained, e.g. in the bed. However, the composition of the fed mixture has a higher impact on the same variable. Another aspect worth to be mentioned is that for higher main gas flow rates, the solid volume fraction in the bed gets similar to the solid volume fraction of the initial mixture. The composition of the fed mixture (dashed lines) and the composition of the mixture that remained in the reactor (full lines) do not differ much. Thus, in this case, the driving force for particle segregation to happen is not strong enough. For this reason, the bed becomes a mixture of both types of particles.

Contrary of what is concluded from Figure 21 (a), in the results shown in Figure 21 (b) the main gas flow rate only influence the fraction of Alumina particles retained for a mixture with 25% of alumina. In this case, it is possible to understand that the percentage of alumina in the bed largely exceeds the amount that was initially present in the feeding vessel. Such results support the conclusions retrieved from the previous plots – alumina, being larger and denser, prevents aluminium from staying inside the chamber. Therefore, the bed will be mainly composed by alumina particles instead of aluminium. Only in the case where the initial amount of alumina is smaller the composition of the fluidized bed goes under 80%. Remark that although the initial compositions are expressed in percentage, the mass value would be the same, since the mixtures fed to the reactor always weighted 100 grams.

By comparing the composition of the mixture fed and the composition of the mixture that composes the bed, the evidence that particle segregation happens in a GSVR is undeniable. The most extreme case is for the initial composition of 25% fluidized with 80 $Nm^3.h^{-1}$ of air. The resulting bed is composed by 70% of alumina, which represents an increase of more than 100% in terms of mass composition. It is clear that this technology has the capacity of segregate particles with different masses. It is also important to remark that this is the most extreme case analyzed in this work. in these circumstances, particles differ both in size and density, which creates a significant difference in terms of mass of each particle. Besides a percentual analysis, the results are also displayed in mass quantity – Figure 22, so that the reader has a clear perception of the real capacity and potential of the setup.

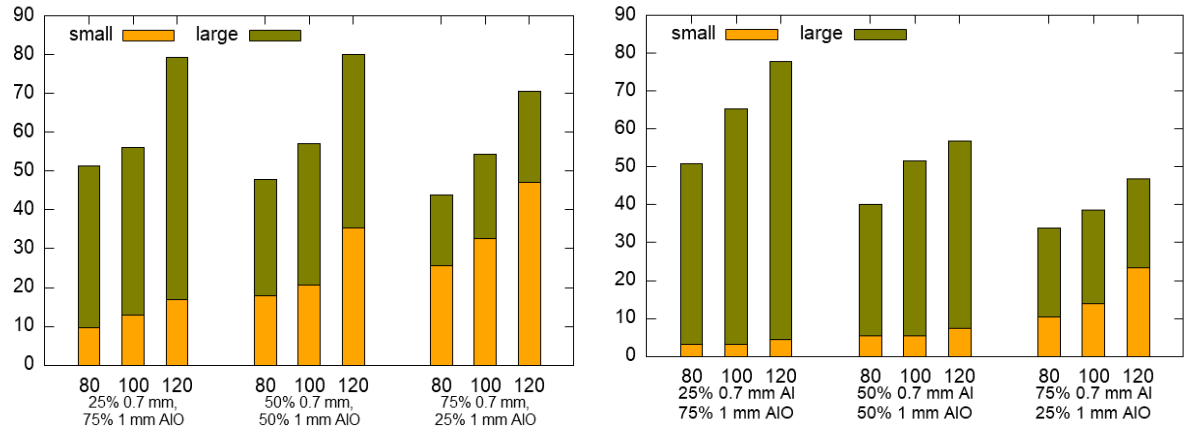

(a) (b)

Figure 22. Composition of the bed in grams for each air flow rate and initial fed mixture. (a) Mixture of alumina of different sizes. (b) Mixture of alumina and aluminium of different sizes.

Figure 22 (a) and (b) have represented a lot of information, which should be carefully analyzed. As mentioned before, the total mass fed to the reactor was always kept constant, at 100 grams, which corresponds to 100%. Hence, the plots should be read according to that principle. If the reader wants to know how much alumina can be fluidized in the GSVR at 80 $Nm^3.h^{-1}$ in a mixture of alumina and aluminium, they should look at the initial composition of the fed mixture and correlate the points (which can have different colors, expect for the case of a binary mixture of 50% each). The results presented are always relative to the initial mass quantity fed from a certain material. Therefore, the red circles and triangles, which correspond to 25 grams of a certain material, will always be found bellow the horizontal line of 25 grams in both graphs.

As already concluded by the percentage plots presented before, when the mixture is composed by particles with different densities and sizes, the maximum loading is larger. These new plots help to understand that the larger the quantity of a certain material in the initial mixture, the larger is the increase of the total mass fluidized, for an increasing air flow rate. This conclusion is clearly seen in Figure 22 (a). In Figure 22 (b), the suggested trend is less notorious, especially for smaller percentages in the initial composition, where the total mass of the material fluidized is practically independent of the gas flow rate.

The following graphs describe how the total amount of solid phase retained in the reactor are affected by the gas flow rate and the composition of the fed mixture. As discussed in Chapter 3, the maximum loading of a GSVR depends much more on the orientation of the exhaust than any other variable. Therefore, the following data is not presented side by side, once it should not be compared like done before. As mentioned before, the maximum loading in a GSVR varies with the composition of the solid phase because of its properties (namely particle size and particle density).

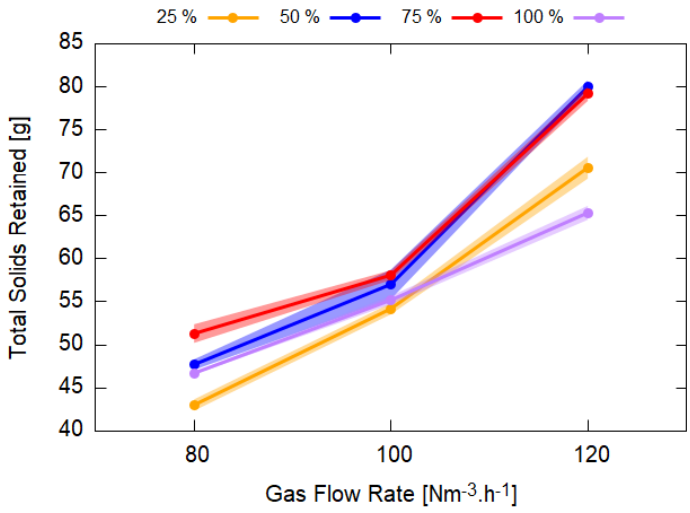

Figure 23. Amount of retained solids for various mixtures with different mass compositions (particle sizes: 1 mm and 0.7-0.8 mm). Colored areas represent respective error region.

Analyzing the relation between the total amount of retained solids and the main gas flow rate imposed, Figure 23 shows a clear dependency on the initial composition and the gas flow rate. Once again, the maximum loading for a pure mixture of 1 mm particles presents itself lower than in most of

the studied cases. Once more, the packing theory is corroborated by experimental data, since it presents a probable explanation for the fact that the maximum loading suffers changes for different feed mixtures. The maximum loading is also seen to improve for higher gas flow rates. A higher amount of gas per hour means a higher amount of momentum to be transferred to the solid phase. Therefore, the amount of particles that the chamber can retain inside increases.

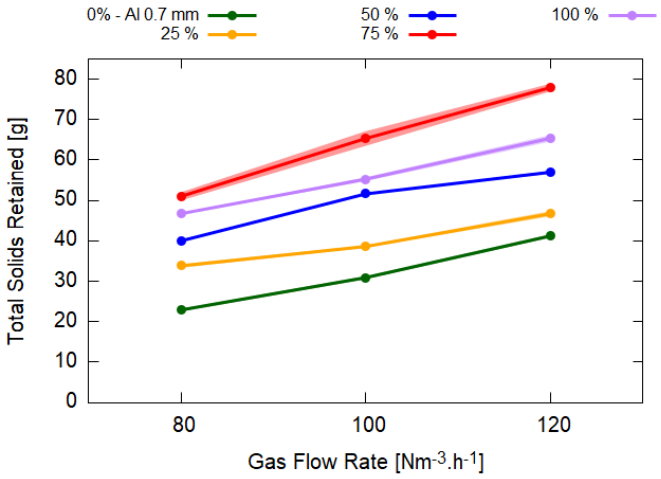

Figure 24. Amount of retained solids for various mixtures with different mass compositions
The different lines represent different mass compositions w.r.t. 1 mm alumina particles. Colored areas represent respective error region.

Comparing the trends between Figure 23 and Figure 24, both sets of mixtures present the same behavior. As the air flow rate increases, the total amount of retained solids (regardless of their nature) rises. As it would be expected, a mixture composed only by aluminium particles with a uniform size has the lowest maximum loading. From the whole spectrum of analyzed particles, these are the lightest and the smallest particles and therefore the hardest to maintain inside the unit. A bed formed by such particles is larger in height but only because the particles are more dispersed in the radial direction. On the other hand, a bed composed only by 1 mm alumina particles is going to be shorter in height, but more compressed, since this material is denser and the particles bigger. Because of the characteristics of the material, the bed itself can hold more mass than the previous case.

Another aspect to be addressed is that the maximum value for the total mass of solids retained in the GSVR is achieved for the initial composition of 75% alumina 1 mm and 25% aluminium 0.7 mm. It is in this situation where it is believed that the packing in the bed is more efficient, meaning that more small particles can be retained in between the big ones. That is a possible explanation for the highest measured values.

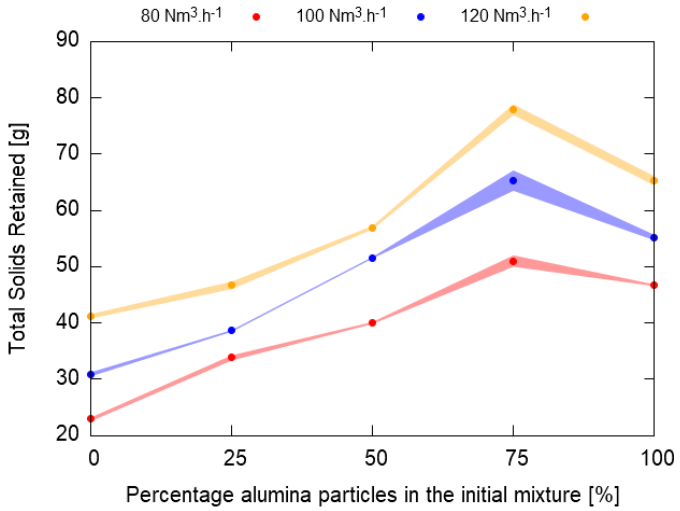

Figure 25. Total solids retained for several gas flow rates. Colored areas represent respective error region.

Figure 25 can be analyzed the same way as Figure 23. The conclusions taken from this picture are the same as the ones mentioned before. The plot can be used to understand the initial composition of the mixture, since the total retained amount depends on it. Once more, the total solids retained is larger for a mixture where the majority of the particles are larger and denser, while the remaining portion is smaller and lighter.

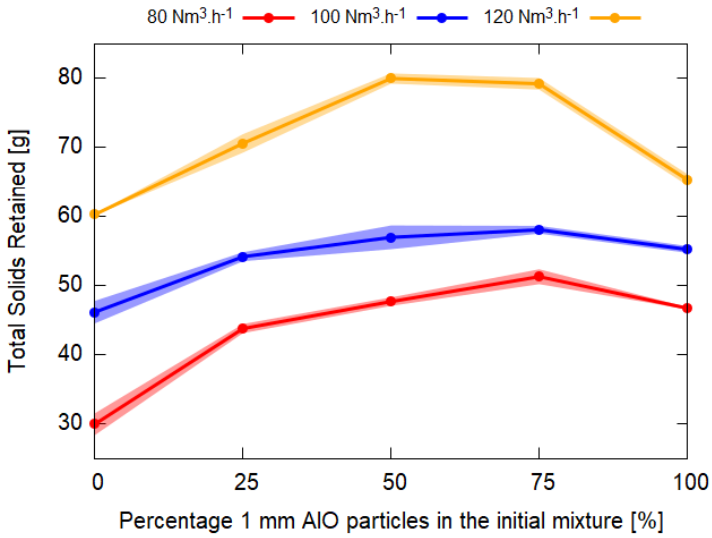

Figure 26. Total solids retained for several gas flow rates (particle sizes: 1 mm and 0.7-0.8 mm). Colored areas represent respective error region.

Figure 26 is perhaps the figure from where we can extract more information. This plot can be used backwards. An Alumina mixture with an unknown composition can be fed to the reactor and the retained percentage will give information regarding its composition, in terms of particle sizes. However, this figure does not reveal any information related to particle segregation. It only shows that for different compositions of the fed mixture, the maximum capacity of the reactor shifts in a non-linear way, without any information about the composition of the bed in each case. As of yet, it was believed that particle segregation in a GSVR was due one of two reasons – different particle diameter or different particle

density, or the combination of those. Now, that hypothesis is at stake. It is believed that the bed packing might influence the particle segregation.

The spaces left empty by larger particles can be occupied by smaller particles, preventing the latter to occupy a smaller radial position inside of the chamber, as it would happen if the bed was only constituted by smaller particles. The fact that the total solids retained is higher for the composition studied which includes the larger quantity of bigger particles gives some positive indication. The outcome arrangement of this mixture provides a higher amount of free spaces for the small particles.

Despite such conclusions, the presented hypothesis can only be confirmed using optical techniques, such as PIV or high-speed camera. Those methods were not available during the period of execution of this master thesis and therefore other strategies were adopted. Pressure drop measurements along the bed and in several points of the reactor were done using the pressure sensors available in the setup – Figure 27. The porosity of the bed was also evaluated by visual measurements of the height of the bed under various set of conditions – Figure 29.

The pressure along the reactor was measured in 14 different spots, every 100 milliseconds. Since we were looking for analyzing the total pressure drop, the data retrieved from sensors PT18 and PT19 is enough for our analysis.

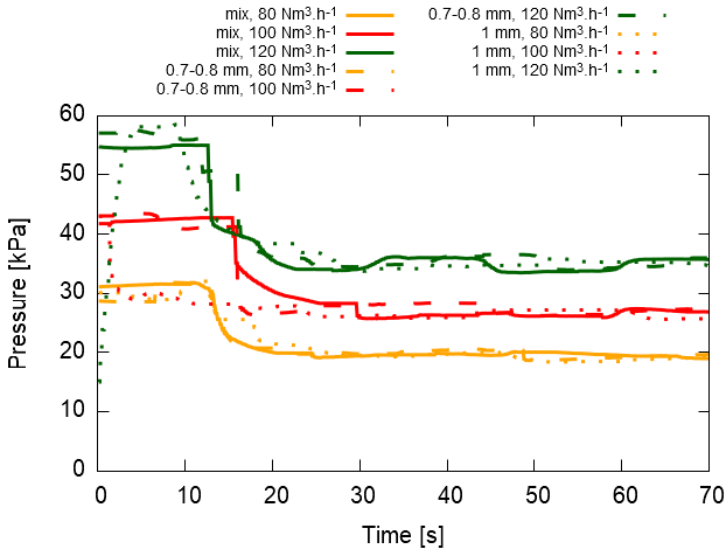

Figure 27. Total pressure drop data for all mixtures and flows used.

In Figure 27, the total pressure drop over time (e.g. during experiments) is displayed. The measurements begin when the air flow rate stabilized in the wanted value and finish after the fluidized bed is stable. For every curve, there are two distinguish zones. The first zone (from 0 to 150) occurs before adding the solids, where the pressure assumes higher values, and the other zone happens when the solids are already rotating inside of the chamber (200 until the end of x axis). By doing an average of the values belonging to each zone, the total pressure drop is determined for each experiment. The next figure compares the averaged total pressure drop for all the evaluated sets of conditions.

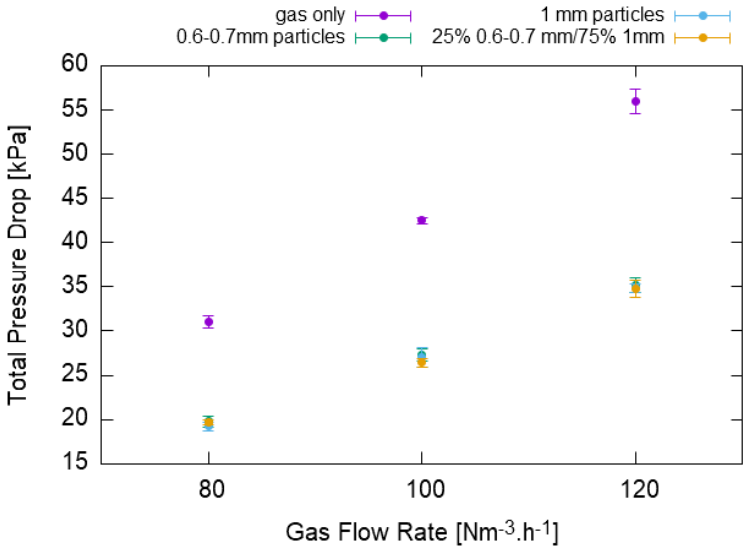

Figure 28. Total pressure drop measured and its errorbars for multiple bed compositions and gas flow rates.

The total pressure drop in a GSVR can be defined as P_{inlet}-P_{outlet}, with pressures being measured before and after the reactor, respectively. Hence, there are two major pressure drop sites to be accounted: the slots and the bed. Because of the reduced width of the slots and the large velocity of the gas through those, the gas loses a lot of momentum, which is converted into a pressure drop for the entire system [68]. The bed is only responsible for a small contribution of the pressure drop. Therefore, the results described in Figure 28 – the total pressure drop being equal for all the analyzed mixtures – do not lead to a particular conclusion, because of the inherently smaller contribution of pressure drop across the bed to the overall pressure drop. Initially, the hypothesis of the same total pressure drop being related with the same packing was considered but after a careful analysis, it got compromised. Hence, by only looking to the data displayed in Figure 28, it is not possible to conclude anything about the degree of mixing or segregation in the bed.

Although such differences, the residence time of the gas phase does not change according to the number of phases present inside the unit. What changes is the residence time distribution of the gas.

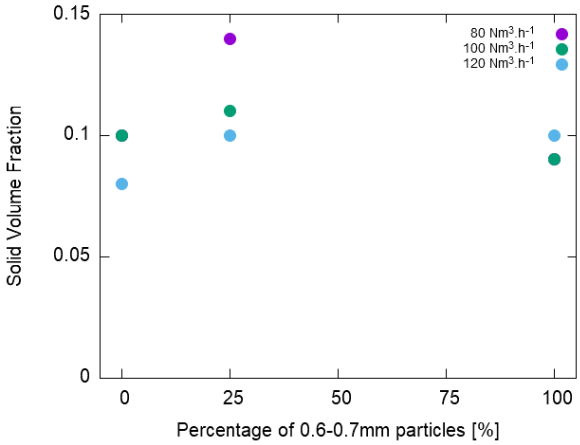

Figure 29. Solid Volume Fraction in the bed under various air flow rates.

By analyzing Figure 29, the void fraction is influenced by with the gas flow rate and the nature of the fed mixture. The higher the gas flow rate, the larger will be the solid volume fraction. Higher flow rates will lead to smaller heights of the bed, which is linked to having higher maximum solid capacities in the reactor for those cases. A higher flow rate will also carry more momentum, which can be distributed to more particles. If those particles achieve the minimum velocity necessary to stay in the bed, the bed will become denser, leading to lower bed lengths and higher solid volume fractions. Although having higher maximum loadings for higher gas flow rates, the expansion of the bed has a bigger effect on the solid volume than the extra amount of particles that can be retained in that case. That is the reason why the solid volume fraction is higher for higher air flow rates. Being the solid volume fraction higher for the mixture between small and large particles, one can assume that the bed is denser in that case and therefore that the packing is more efficient.

To conclude this topic, quantitative information regarding the degree of mixing or segregation was collected and several attempts were made to gather more information about the subject. Those efforts were based in experimental measurements done with the available resources at that time. Unfortunately, none of the techniques included visualization of the fluidized bed, which could be achieved using PIV or high speed camera. Observing the bed during fluidization is crucial to understand better this topic and to confirm some of the assumptions done in these last pages.

Although these unfortunate circumstances, there are some conclusions worth to be mentioned. Both particle segregation and mixing, in several degrees, were observed while operating the setup. When the driving force for particle segregation, e.g. difference in particle mass, due to different densities and sizes, is strong enough, the composition of the entrained quantity follows a trend. Heavier particles tend to stay inside the chamber, rotating in the fluidized bed and in the freeboard region, while lighter particles are entrained easily, hence representing the larger portion of the entrained quantity. This situation was observed when different materials – Alumina and Aluminium – with different sizes were fed in a binary mixture to the unit.

When the difference between masses of both sets of particles is not big enough, the difference in terms of composition of the entrained and retained quantities are less notorious. Although the radial position of each set of particles is different, that difference is not strong enough to enable particle segregation. Therefore, particle mixing in the bed is the most rightful way to describe the behavior of the solid phase subjected to fluidization in a GSVR, in the range of gas flow rate studied. To corroborate this hypothesis, some positive indications were found during this study. The smaller void fraction of the bed when particles of different sizes are present indicates a changing in the arrangement of the bed. Such measurement can be correlated with a more efficient packing. Once more, the reader should be reminded that there was no visual confirmation of the packing. This conclusion is merely a way to justify the obtained results.

All the results and conclusions presented in this chapter are in agreement with a published article in the same matter[45]. Weber et al. present several sets of experiments where different materials, with different sizes, are fed to a GSVR and the segregation and mixing degrees are evaluated. That

evaluation accounts with visual technique, namely PIV, but only for the case where segregation occurs. The conclusions retrieved from that work are similar to the ones already mentioned before.

6. Conclusions and Future Work

The lack of knowledge reported on literature regarding the hydrodynamics in a GSVR is keeping such technology away from the industrial world. Its characteristics, such as the ease of use and operation of the unit, in which is possible to conduct a complete experiment in less than 20 minutes (including cleaning) and its value towards process intensification are mandatory for improving an industrial process.

There were 4 clear aspects which were to be depicted in this dissertation. Those were studying the maximum loading of the unit and the degree of segregation/mixing of the solid phase, experimentally, a theoretical model to understand which materials and sizes can be successfully processed in the unit and designing a Geldart-kind classification for the GSVR. Unfortunately, the last one of the objectives was not executed. There was not enough time or means (it is necessary a considerable variety of material, with different sizes and densities) to meet that objective. In the future, an attempt to adapt the current Geldart classification should be done. Even though there are already some classifications which are valid under centrifugal forces, none of the reported ones is straightforward enough to be used in the daily life, as it happens with the original Geldart classification.

The larger maximum loading (by three times) was achieved for such a configuration where the exhaust is orientated against the gravity. When the exhaust is against gravity, it is possible that a portion of the particles that cannot achieve enough velocity to keep rotating in the bed, fall on the bottom plate of the reactor. This phenomenon will lead to erroneous values of maximum loading, since, by definition, the maximum loading of a GSVR is the maximum mass of solid phase that can be successfully fluidized using a certain flow of gas phase. Beyond that value, all the particles fed will be entrained from the chamber. If the particles end up falling instead of entrained, the measured value of the maximum loading will be inaccurate. This situation and its extent could not be verified by neither of the students, but its occurrence must be accounted due to the experimental observations. Next studies on the subject can focus on the reported phenomenon. A measurement of its extent should be done.

The segregation/mixing of the solid phase is a subject reported in the literature, but lack of information exists when it comes to its extent. The trials done lead to conclude that only a major difference between the mass of the particles will cause a significant particle segregation, e.g. smaller/lighter particles will be entrained while larger/heavier ones will be retained in the unit. To achieve such conclusion, particles with different sizes and densities were used, to magnify the difference between masses. The effect of the mass composition of the fed mixture was also evaluated. The percentage of smaller/lighter particles has a negative impact on the maximum loading, making it smaller. Differences on the amount of particles retained in the chamber can also be related with the packing of the particles. This factor is believed to be optimum for a mixture of 75% alumina 1 mm and 25% aluminium 0.7 mm. However, this hypothesis can only be verified once visual methods are used to evaluate the arrangement of the bed. Such experiments brought a new understanding of how particle segregation/mixing work in a fluidized bed inside a GSVR. In the future, visual techniques must be

performed while fluidizing materials with different sizes and densities so that all the explanations for particle segregation/mixing reported in this document may be validated or discarded. Nonetheless, the experimental dataset gathered about segregation (or mixing) can also be useful in future for validation of CFD simulations involving a binary solids fluidization in vortex devices.

Besides experiments, this thesis also reports a portion of modeling work. This mathematical model strives to predict the minimum size of a particle with a certain density that can be fluidized in a GSVR. As reported before, this model was successfully built, since its conclusions are supported by published articles but presents considerable limitations on the virtue of simplifications/assumptions made during its development. Mathematical limitations arise in the iterative process, which can converge to solutions other than the trivial one if and only if a specific drag coefficient correlation is used. The second limitation has to do with the short range of situations where the model can be employed. The model should only be extended to materials with a similar fluidization behavior (under centrifugal forces) to aluminum, e.g. that belongs to the same group in the Geldart classification. The need of accurate azimuthal solid velocities can also be a barrier to obtaining good results from the model. Despite of these constrains, the modeling work proved to be useful for predicting which materials of what size can be processed in a certain unit and for designing purposes. This model gives a different perspective (more theorical) than the preformed experiments. In the future, the outcoming results of the model can be compared with experiments or even simulations. Those comparisons will lead to a refinement of the model itself, so it can represent the reality to a better extent. The referred limitations, mainly the mathematical ones, should be studied and a solution for the convergence problem obtained. The answer to solve such problem can be related with the software used for the iterative process. A more powerful tool, such as Matlab or Python may approach the problem by using another method and therefore achieve new solutions, which proved to be beyond the scope of this thesis.

To conclude, this dissertation strives to fill a part of the gap in the vortex literature regarding the hydrodynamics of a GSVR. The optimum configuration for the setup is reported in terms of maximum loading, as well as the degree of segregation/mixing of the solid phase. Such knowledge will lead to an operation much more efficient than before. A larger maximum loading will lead to a larger quantity of materials processed during the same period of time and the understanding of the segregation phenomenon will be useful in processes where a decrease of the particle size happens, such as drying or pyrolysis, where formation of ash occurs.

7. References

(1) Gilliland, E.; Mason, E. Gas and solid mixing in fluidized beds. *Industrial & Engineering Chemistry* **1949,** *41* (6), 1191.

(2) Ergun, S.; Orning, A. A. Fluid flow through randomly packed columns and fluidized beds. *Industrial & Engineering Chemistry* **1949,** *41* (6), 1179.

(3) Daud, W. R. W. Fluidized bed dryers—Recent advances. *Advanced Powder Technology* **2008,** *19* (5), 403.

(4) De Wilde, J. Gas–solid fluidized beds in vortex chambers. *Chemical Engineering Processing: Process Intensification* **2014,** *85*, 256.

(5) Gel'perin, N.; Ainstein, V.; Gakman, I. Rate of inception of fluidization and expansion of a fluidized layer in a centrifugal force field. *Khim. Mash.* **1964,** (5), 18.

(6) Dongbang, W.; Pirompugd, W.; Triratanasirichai, K. The drying kinetics of chilies using a rotating fluidized bed technique. *American Journal of Applied Sciences* **2010,** *7* (12), 1599.

(7) Eliaers, P.; de Broqueville, A.; Poortinga, A.; van Hengstum, T.; De Wilde, J. High-G, low-temperature coating of cohesive particles in a vortex chamber. *Powder Technology* **2014,** *258*, 242.

(8) Hirsch, D.; Steinfeld, A. Solar hydrogen production by thermal decomposition of natural gas using a vortex-flow reactor. *International Journal of Hydrogen Energy* **2004,** *29* (1), 47.

(9) Eliaers, P.; De Wilde, J. Drying of biomass particles: Experimental study and comparison of the performance of a conventional fluidized bed and a rotating fluidized bed in a static geometry. *Drying technology* **2013,** *31* (2), 236.

(10) De Wilde, J.; Richards, G.; Benyahia, S. Qualitative numerical study of simultaneous high-G-intensified gas–solids contact, separation and segregation in a bi-disperse rotating fluidized bed in a vortex chamber. *Advanced Powder Technology* **2016,** *27* (4), 1453.

(11) Schuerewegen, C.; Heynderickx, G. p.; Van Geem, K. c. "Experimental Heat Transfer Studies in a Hot Flow Vortex Reactor," University of Gent, 2018.

(12) Kulkarni, S. R.; Gonzalez-Quiroga, A.; Nuñez, M.; Schuerewegen, C.; Perreault, P.; Goel, C.; Heynderickx, G. J.; Van Geem, K. M.; Marin, G. B. J. A. J. An experimental and numerical study of the suppression of jets, counterflow and backflow in vortex units. *AIChE Journal*, e16614.

(13) Kovacevic, J.; Pantzali, M.; Heynderickx, G.; Marin, G. Bed stability and maximum solids capacity in a Gas–Solid Vortex Reactor: Experimental study. *Chemical Engineering Science* **2014,** *106*, 293.

(14) Ekatpure, R.; Suryawanshi, V.; Heynderickx, G.; De Broqueville, A.; Marin, G. Experimental investigation of a gas–solid rotating bed reactor with static geometry. *Chemical Engineering Processing: Process Intensification* **2011,** *50* (1), 77.

(15) Chen, Y. M. Fundamentals of a centrifugal fluidized bed. *AIChE Journal* **1987,** *33* (5), 722.

(16) Nakamura, H.; Watano, S. Numerical modeling of particle fluidization behavior in a rotating fluidized bed. *Powder Technology* **2007,** *171* (2), 106.

(17) Kao, J.; Pfeffer, R.; Tardos, G. On partial fluidization in rotating fluidized beds. *AIChE Journal* **1987,** *33* (5), 858.

(18) Watano, S.; Nakamura, H.; Hamada, K.; Wakamatsu, Y.; Tanabe, Y.; Dave, R. N.; Pfeffer, R. Fine particle coating by a novel rotating fluidized bed coater. *Powder Technology* **2004,** *141* (3), 172.

(19) Eliaers, P.; Pati, J. R.; Dutta, S.; De Wilde, J. Modeling and simulation of biomass drying in vortex chambers. *Chemical Engineering Science* **2015,** *123*, 648.

(20) Qian, G. H.; Bagyi, I.; Burdick, I. W.; Pfeffer, R.; Shaw, H.; Stevens, J. G. Gas–solid fluidization in a centrifugal field. *AIChE Journal* **2001,** *47* (5), 1022.

(21) Qian, G. H.; B´ gyi, I. n.; Pfeffer, R.; Shaw, H.; Stevens, J. G. Particle mixing in rotating fluidized beds: inferences about the fluidized state. *AIChE Journal* **1999,** *45* (7), 1401.

(22) "Particle Image Velocimetry "https://velocimetry.net/principle.htm 03/05/2019.

(23) Kovacevic, J. Z.; Pantzali, M. N.; Niyogi, K.; Deen, N. G.; Heynderickx, G. J.; Marin, G. B. J. C. E. S. Solids velocity fields in a cold-flow gas–solid vortex reactor. *Chemical Engineering Science* **2015,** *123*, 220.

(24) "Measurement Principles of PIV,"https://www.dantecdynamics.com/measurement-principles-of-piv, 03/05/2019.

(25) Kulkarni, S. R.; Vandewalle, L. A.; Gonzalez-Quiroga, A.; Perreault, P.; Heynderickx, G. J.; Van Geem, K. M.; Marin, G. B. Computational fluid dynamics-assisted process intensification study for biomass fast pyrolysis in a gas–solid vortex reactor. *Energy Fuels* **2018,** *32* (10), 10169.
(26) Ding, Y.; Forster, R.; Seville, J.; Parker, D. Scaling relationships for rotating drums. *Chemical Engineering Science* **2001,** *56* (12), 3737.
(27) Niyogi, K.; Torregrosa, M. M.; Pantzali, M. N.; Heynderickx, G. J.; Marin, G. B.; Shtern, V. N. On near-wall jets in a disc-like gas vortex unit. *AIChE Journal* **2017,** *63* (5), 1740.
(28) Brossard, C.; Monnier, J.; Barricau, P.; Vandernoot, F.-X.; Le Sant, Y.; Champagnat, F.; Le Besnerais, G. Principles and applications of particle image velocimetry. *AerospaceLab* **2009,** (1), p. 1.
(29) "Planar laser-induced fluorescence,"https://en.wikipedia.org/wiki/Planar_laser-induced_fluorescence, 02/05/2019.
(30) Liu, Z.; Hitimana, E.; C. Hill, J.; Fox, R.; Olsen, M. Turbulent Mixing in the Confined Swirling Flow of a Multi-Inlet Vortex Reactor. *AIChE Journal* **2017,** *63*.
(31) Liu, Z.; Fox, R. O.; Hill, J. C.; Olsen, M. G. A Batchelor Vortex Model for Mean Velocity of Turbulent Swirling Flow in a Macroscale Multi-Inlet Vortex Reactor. *Journal of Fluids Engineering* **2015,** *137* (4), 041204.
(32) Feng, H.; Olsen, M.; Liu, Y.; Fox, R.; C. Hill, J. Investigation of Turbulent Mixing in a Confined Planar-Jet Reactor. *AIChE Journal* **2005,** *51*, 2649.
(33) Pantzali, M. N.; Kovacevic, J. Z.; Heynderickx, G. J.; Marin, G. B.; Shtern, V. N. Radial pressure profiles in a cold-flow gas-solid vortex reactor. *AIChE Journal* **2015,** *61* (12), 4114.
(34) Ashcraft, R. W.; Heynderickx, G. J.; Marin, G. B. Modeling fast biomass pyrolysis in a gas–solid vortex reactor. *Chemical Engineering Journal* **2012,** *207*, 195.
(35) Cabrera, M. A.; Wu, W. Experimental modelling of free-surface dry granular flows under a centrifugal acceleration field. *Granular Matter* **2017,** *19* (4), 78.
(36) Cook, C. A.; Cundy, V. A. Heat transfer between a rotating cylinder and a moist granular bed. *International journal of heat mass transfer* **1995,** *38* (3), 419.
(37) Chaudhuri, B.; Muzzio, F. J.; Tomassone, M. S. Modeling of heat transfer in granular flow in rotating vessels. *Chemical Engineering Science* **2006,** *61* (19), 6348.
(38) Dewettinck, K.; Huyghebaert, A. Fluidized bed coating in food technology. *Trends in Food ScienceTechnology* **1999,** *10* (4-5), 163.
(39) Ashcraft, R. W.; Kovacevic, J.; Heynderickx, G. J.; Marin, G. B. Assessment of a Gas–Solid Vortex Reactor for SO2/NO x Adsorption from Flue Gas. *Industrial Engineering Chemistry Research* **2013,** *52* (2), 861.
(40) Dodson, C. E.; Lakshmanan, V. I. An innovative gas-solid torbed reactor for the recycling industries. *JOM* **1998,** *50* (7), 29.
(41) "TORBED Compact Bed Reactor ('CBR'), TORBED Reactor Technology for Gas Solid Contact Processes,"www.torftech.com, 2017.
(42) Shi, M.; Wang, H.; Hao, Y. Experimental investigation of the heat and mass transfer in a centrifugal fluidized bed dryer. *Chemical Engineering Journal* **2000,** *78* (2-3), 107.
(43) Kamranian Marnani, A.; Bück, A.; Antonyuk, S.; van Wachem, B.; Thévenin, D.; Tomas, J. The Effect of the Presence of Very Cohesive Geldart C Ultra-Fine Particles on the Fluidization of Geldart A Fine Particle Beds. *Processes* **2019,** *7* (1), 35.
(44) Verma, V.; Li, T.; De Wilde, J. Coarse-grained discrete particle simulations of particle segregation in rotating fluidized beds in vortex chambers. *Powder Technology* **2017,** *318*, 282.
(45) Weber, J. M.; Stehle, R. C.; Breault, R. W.; De Wilde, J. Experimental study of the application of rotating fluidized beds to particle separation. *Powder Technology* **2017,** *316*, 123.
(46) "What is Process Intensification and How Can You Implement It?,"https://www.epicmodularprocess.com/blog/what-is-process-intensification, 27/03/2019.
(47) Wang, H.; Mustaffar, A.; Phan, A. N.; Zivkovic, V.; Reay, D.; Law, R.; Boodhoo, K. A review of process intensification applied to solids handling. *Chemical Engineering Processing: Process Intensification* **2017,** *118*, 78.
(48) Geldart, D. Types of gas fluidization. *Powder Technology* **1973,** *7* (5), 285.
(49) "ZSM-5,"https://en.wikipedia.org/wiki/ZSM-5, 01/04/2019.
(50) "The Essential Chemical Industry – online – Calcium Carbonate. ,"http://www.essentialchemicalindustry.org/chemicals/calcium-carbonate.html 04/04/2019.
(51) Dahmash, E. Z.; Mohammed, A. R. Functionalised particles using dry powder coating in pharmaceutical drug delivery: promises and challenges. *Expert opinion on drug delivery* **2015,** *12* (12), 1867.

(52) Ye, M.; van der Hoef, M. A.; Kuipers, J. A numerical study of fluidization behavior of Geldart A particles using a discrete particle model. *Powder Technology* **2004,** *139* (2), 129.
(53) Ye, M.; van der Hoef, M. A.; Kuipers, J. The effects of particle and gas properties on the fluidization of Geldart A particles. *Chemical Engineering Science* **2005,** *60* (16), 4567.
(54) Matsuda, S.; Hatano, H.; Tsutsumi, A. Ultrafine particle fluidization and its application to photocatalytic NOx treatment. *Chemical Engineering Journal* **2001,** *82* (1-3), 183.
(55) Piepers, H.; Cottaar, E. J. E.; Verkooijen, A.; Rietema, K. Effects of pressure and type of gas on particle-particle interaction and the consequences for gas—solid fluidization behaviour. *Powder Technology* **1984,** *37* (1), 55.
(56) Yang, W.-C. Modification and re-interpretation of Geldart's classification of powders. *Powder Technology* **2007,** *171* (2), 69.
(57) Yehuda, T.; Kalman, H. 18th International Conference on Transport; p 401.
(58) Gündoğdu, Ö.; Tüzün, U. Gas Fluidisation of Nano-particle Assemblies: Modified Geldart classification to account for multiple-scale fluidisation of agglomerates and clusters. *KONA Powder Particle Journal* **2006,** *24*, 3.
(59) Hakim, L. F.; Portman, J. L.; Casper, M. D.; Weimer, A. W. Aggregation behavior of nanoparticles in fluidized beds. *Powder Technology* **2005,** *160* (3), 149.
(60) Valverde, J. M.; Castellanos, A. Effect of vibration on agglomerate particulate fluidization. *AIChE Journal* **2006,** *52* (5), 1705.
(61) van Ommen, J. R.; Valverde, J. M.; Pfeffer, R. Fluidization of nanopowders: a review. *Journal of nanoparticle research : an interdisciplinary forum for nanoscale science and technology* **2012,** *14* (3), 737.
(62) Dukhin, S.; Zhu, C.; Dave, R. N.; Yu, Q. Hydrodynamic fragmentation of nanoparticle aggregates at orthokinetic coagulation. *Advances in colloid and interface science* **2005,** *114-115*, 119.
(63) Morrison, F. A. *An Introduction to Fluid Dynamics*; Cambridge University Press: New York, 2013.
(64) Gonzalez-Quiroga, A.; Kulkarni, S. R.; Vandewalle, L.; Perreault, P.; Goel, C.; Heynderickx, G. J.; Van Geem, K. M.; Marin, G. B. Azimuthal and radial flow patterns of 1g-Geldart B-type particles in a gas-solid vortex reactor. *Powder Technology* **2019**.
(65) Gonzalez-Quiroga, A.; Reyniers, P. A.; Kulkarni, S. R.; Torregrosa, M. M.; Perreault, P.; Heynderickx, G. J.; Van Geem, K. M.; Marin, G. B. Design and cold flow testing of a Gas-Solid Vortex Reactor demonstration unit for biomass fast pyrolysis. *Chemical Engineering Journal* **2017,** *329*, 198.
(66) Friedle, M.; Niyogi, K.; Torregrosa, M. M.; Marin, G. B.; Heynderickx, G. J. A drag model for the gas-solid vortex unit. *Powder Technology* **2017,** *312*, 210.
(67) P. Rowe, G. H. Drag Forces in a Hydraulic Model of a Fluidised bed. *Trans. Instn. Chem. Engrs.* **1960**.
(68) Kulkarni, S. R.; Gonzalez-Quiroga, A.; Nuñez, M.; Schuerewegen, C.; Perreault, P.; Goel, C.; Heynderickx, G. J.; Van Geem, K. M.; Marin, G. B. An experimental and numerical study of the suppression of jets, counterflow and backflow in vortex units. *AIChE Journal* **2019**, e16614.